International Journal of Fracture **80:** 103–145, 1996.

Basic issues in the mechanics of high cycle metal fatigue

DAVID L. McDOWELL
G.W. Woodruff School of Mechanical Engineering, School of Materials Science and Engineering, Georgia Institute of Technology, Atlanta, GA 30332-0405, USA

Received 17 January 1996; accepted in revised form 30 July 1996

Abstract. Mechanics issues related to the formation and growth of cracks ranging from subgrain dimension to up to the order of one mm are considered under high cycle fatigue (HCF) conditions for metallic materials. Further efforts to improve the accuracy of life estimation in the HCF regime must consider various factors that are not presently addressed by traditional linear elastic fracture mechanics (LEFM) approaches, nor by conventional HCF design tools such as the S-N curve, modified Goodman diagram and fatigue limit. A fundamental consideration is that a threshold level for ΔK for small/short cracks may be considerably lower than that for long cracks, leading to non-conservative life predictions using the traditional LEFM approach.

Extension of damage tolerance concepts to lower length scales and small cracks relies critically on deeper understanding of (a) small crack behavior including interactions with microstructure, (b) heterogeneity and anisotropy of cyclic slip processes associated with the orientation distribution of grains, and (c) development of reliable small crack monitoring techniques. The basic technology is not yet sufficiently advanced in any of these areas to implement damage tolerant design for HCF. The lack of consistency of existing crack initiation and fracture mechanics approaches for HCF leads to significant reservations concerning application of existing technology to damage tolerant design of aircraft gas turbine engines, for example. The intent of this paper is to focus on various aspects of the propagation of small cracks which merit further research to enhance the accuracy of HCF life prediction. Predominant concern will rest with polycrystalline metals, and most of the issues pertain to wide classes of alloys.

1. Introduction: historical perspective of the mechanics of metal fatigue

Studies of the fatigue limit of steels can be traced back approximately 150 years. For nearly a century, the problem of low amplitude HCF was of primary concern. Empirical S-N approaches were established as state-of-the-art in HCF design/analysis as a tool for fatigue life correlation/prediction. These approaches, established prior to the development of fracture mechanics, acknowledged the eventual formation of cracks and 'failure' without addressing crack growth or failure conditions in detail. Primary concerns involved effects of surface finish, residual stress, mean stress, and variability of fatigue strength or life.

The focus of the fledgling field of fracture mechanics in the 1940s and 1950s was directed at static fracture problems. Later, identification of relations between da/dN and ΔK for long cracks [1] eventually led to design against fatigue crack propagation (FCP) and damage tolerance concepts. The more venerate subject of S-N curves and fatigue limits for notched components evolved into local stress-life and strain-life approaches for 'crack initiation' which increasingly focused on finite life design and low cycle fatigue (LCF) in the 1960s, driven by aerospace and automotive applications. Strain-life relations [2–3] were developed to correlate strain amplitude with LCF crack initiation life. During this era, the disciplines of crack initiation and crack propagation were largely viewed as distinct, and largely remain so today in engineering practice. In the 1970s, approaches were developed to bridge initiation and propagation mechanics by applying the local stress- or strain-life approach at notches to predict the development of a crack of specified length, with subsequent propagation treated

by fracture mechanics [4–5]. Crack initiation and propagation were viewed as serial processes with independent mechanics treatments, forming the basis for prediction of *total* fatigue life.

Scientific curiosity, enhancements of detection capabilities, and economic necessity have driven the application of fracture mechanics concepts to ever shorter cracks within the last 10–15 years. This era has been accompanied by an explosion of computer-controlled, servo-hydraulic testing capability, along with advancements of hardware and software for imaging small cracks. Much of this work has been conducted at reasonably high stress amplitudes. While the long crack data have suggested the existence of threshold behavior, observations of small cracks consistently violate this notion; they exhibit a more rapid growth rate than predicted by extrapolation of long crack data based on ΔK and grow below the long crack threshold, $\Delta K_{th\infty}$. Hence, an 'anomaly' emerged from the perspective of fracture mechanics. Of course, this anomalous small crack behavior is the intended domain of application of the S-N curve and local stress- or strain-life relations.

As the small cracks under consideration approached microstructural dimensions, the boundary between initiation mechanics and propagation mechanics became blurred. Treatment of the sequential processes of nucleation of cracks of microscopic dimensions (e.g. μm) followed by incremental propagation emerged as an objective. Small crack HCF behavior has not received the same level of basic research that has been devoted to LCF conditions. This is due in part to the tedious nature of such experiments and difficulty in monitoring crack growth under these conditions. Since cracks remain small in HCF for most of the fatigue life of smooth or notched specimens, long crack behavior has less relevance. Consequently, HCF design practice still has no well-established foundation for incorporation of fracture mechanics principles. Hence, tools such as the S-N curve, Goodman diagram, and the local stress-life approach still form the basis of HCF design.

This paper discusses many of the issues related to expanding the foundation for modeling the HCF problem based on the propagation of small cracks at various scales, ranging from microstructural to structural dimensions. A progression of events lead to fatigue failure: early stages of crack formation (nucleation), small crack growth and then propagation of mechanically long cracks. A myriad of possibilities exist for the nucleation of cracks, including formation of persistent slip bands, pre-existing defects associated with processing, in-service fretting and foreign object damage (significant in fatigue of airfoils and gas turbine components), etc. Each of these topics are characterized by their own disciplinary literature and are subject to enormous variability associated with material, loading conditions, etc. They essentially represent different sorts of incubation periods, boundary conditions, and initial crack lengths and orientations for propagation analyses. This paper will instead focus on rather more universally-encountered mechanics aspects of small crack growth behavior that represent a challenge to the unification of crack initiation and propagation approaches, severely testing the limits of applicability of each. This is discussed at length in Section 2.

The role of microstructure in small crack growth is highlighted in Section 3. Section 4 considers the essential dependence of local mode mixity on the applied multiaxial stress state. Relatively more brief treatment is afforded notch effects on small crack propagation (Section 5) and amplitude sequence and mean stress effects (Section 6) in HCF. Environment and time-dependent effects are potentially quite significant in HCF, owing to the proximity of free surfaces; Section 7 presents only a general discussion of these topics. Since these effects also tend to be quite specific to material system and operating environment, this paper will not consider them in greater detail. The reader is instead referred to other literature concerning particular alloys of interest. Likewise, surface treatments such as media finishing,

coating, and shotpeening are of enormous practical significance to industrial applications and play a prominent role in tailoring HCF resistance of components. Basic investigations are necessary to shed light on the precise mechanisms of retardation of crack formation and growth associated with these surface treatments. However, due to ambiguities in present HCF initiation and propagation approaches and inadequate representation of mean stress and sequence effects, even in the absence of such surface treatments, the more fundamental, isolated microstructure/mechanics aspects of small crack propagation behavior are addressed here.

2. Distinguishing features of small crack propagation

A popular, heuristic decomposition of total life is given by

$$N_T = N_i + N_p, \tag{1}$$

where N_i (alternatively termed N_f) is the number of cycles to 'initiation' of a crack-like defect and N_p is the number of cycles of propagation to critical dimension. Classically, N_p is assessed using LEFM concepts. The initiation life N_i is estimated using various approaches ranging from local stress-life approaches for HCF to the Coffin-Manson equation for LCF, or hybrid approaches, such as the local strain-life equation, which combine these two over the full range of lives. The number of cycles to crack initiation typically relates to the formation of small cracks on the order of 0.5 mm to 2 mm in length. Such flaws are detectable. The label 'initiation life' is somewhat misleading since it includes processes of nucleation as well as the propagation of small cracks, alternatively termed as microcracks. In design for damage tolerance, the presence of an initial defect is assumed a priori, and inspection intervals are set according to the application of propagation mechanics. Crack initiation mechanics are of little use for this purpose. This is a viable approach in structures where flaws can be monitored in critical locations, and where crack growth conforms to a well-established propagation law. In contrast, the initiation and growth of small cracks in reciprocating or rotary machinery subjected to HCF loading conditions may not be evident for the great majority of total life, and in many cases the N_i term in (1) is dominant. The propagation behavior of small cracks during the 'initiation' phase is unfortunately not as well-characterized as that of long cracks.

An important aspect of HCF is the quantification of the relation between the macroscopic applied stress state and the microscopic or local stress state in the vicinity of certain surface features such as surface roughness, micronotches, or individual crystalline regions or grains. An assumed homogeneous stress state at the macroscopic scale is accompanied by a highly heterogeneous orientation distribution of grains and of local cyclic plastic slip processes at the scale of grains. This situation is illustrated in Figure 1. Heterogeneity manifests itself in statistical variations of the so-called fatigue strength in HCF. It is commonly observed that the scatter in fatigue life for a given stress amplitude increases markedly with life until it is several orders of magnitude under HCF conditions, as shown in Figure 1. Weibull statistics have been introduced to quantify the variation of fatigue strength under HCF conditions, but such variations have not heretofore been quantitatively correlated with microstructure variation or distribution of microplasticity. The smooth specimen fatigue limit is known to depend on various factors including surface residual stresses, surface roughness and hardness, distribution of second phase particles, and so on. In some materials (e.g. Al alloys), a fatigue limit may not exist. Even in steels, it may be eradicated by a single overload or sequences involving overloads [6]. While LCF behavior is dominated by the propagation of cracks at

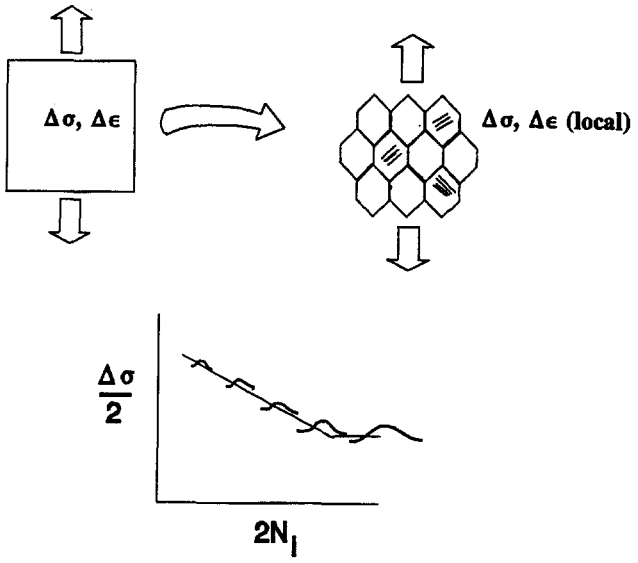

Figure 1. Homogeneous idealization (top left) and actual heterogeneous distribution of cyclic slip (top right); scatter increases with increasing fatigue life (bottom).

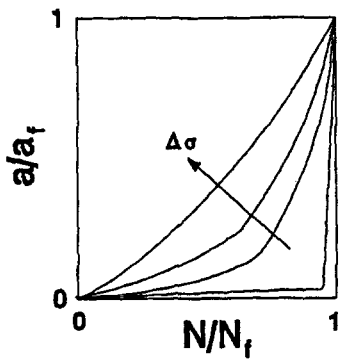

Figure 2. Representative nonlinear evolution of normalized crack length (a_f = final crack length) as a function of normalized cycles.

various scales, design against HCF focuses on various mechanisms which may lead to crack arrest, i.e. quantification of thresholds of applied stress or driving force below which cracks no longer will grow.

Another key feature of HCF behavior is that of strong sequence effects, particularly for sequences of high and low amplitude cycles. In such cases, the simple Palmgren–Miner linear damage rule based on cycle fraction summation breaks down as a criterion for cumulative damage. This breakdown may be understood in the context of the nonlinearity of the growth of small cracks with number of cycles under constant amplitude uniaxial loading conditions, shown schematically in Figure 2. This presentation of crack length versus cycles is primal in nature, separate from any particular theoretical interpretation. Low stress amplitudes lead to highly nonlinear progression of crack length with fatigue life, with increasing stress amplitudes tending towards a higher degree of linearity. Sufficiently low amplitudes can lead to deceleration and arrest of crack growth. Therefore, Miner's rule might be expected to be

Figure 3. Differences in cyclic microslip and microcrack distribution in LCF (left) and HCF (right) for macroscopically homogeneous cyclic straining.

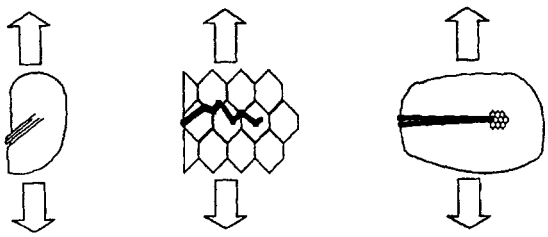

Figure 4. Progression of length scales in fatigue: (a) nucleation at PSBs or pre-existing defects, (b) crack length on the order of microstructure, and (c) long crack behavior.

more accurate for sequences of relatively high amplitude cycles, whereas cumulative damage for sequences of HCF and LCF amplitudes might be quite inaccurately predicted. Further consideration of crack nucleation processes introduces additional nonlinearity and potential sequence effects.

A distinguishing feature of HCF is the high degree of heterogeneity of local cyclic slip processes. Microcrack distribution is also highly heterogeneous in homogenous macroscopic cyclic deformation states, as schematically shown in Figure 3. Under high amplitude cycling (LCF), persistent slip bands and microcracks are fairly uniformly distributed among grains, leading to low variability of fatigue crack nucleation and propagation processes. There is a regime of crystallographic growth of microcracks roughly coincident with the orientation of maximum shear planes, termed by Forsyth [7] as Stage I growth. For low stress amplitudes (HCF), the cyclic plastic slip processes are highly heterogeneously distributed among grains and surface crack density is sparse. There may also be an early transition to Stage II behavior, characterized by propagation normal to the direction of the maximum principal stress range. Persistent slip band (PSB) spacing and spacing of nucleated small cracks decreases with increasing strain amplitude. Typically, only a single dominant flaw ultimately propagates to failure in HCF and the crack density is relatively low in smooth specimens compared to the LCF case. There is a corresponding increase of scatter of fatigue strength under HCF conditions linked to this increasing heterogeneity.

Fatigue crack nucleation and growth occurs along a progression of length scales ranging from the order of 1 μm to the scale of individual grains, to long crack behavior where the scale of individual grains (50 μm–100 μm) is small compared to the crack length and the characteristic length scale for crack tip damage or the cyclic plastic zone, as illustrated in Figure 4. Each of these three scales corresponds to distinct mechanics treatments. Although

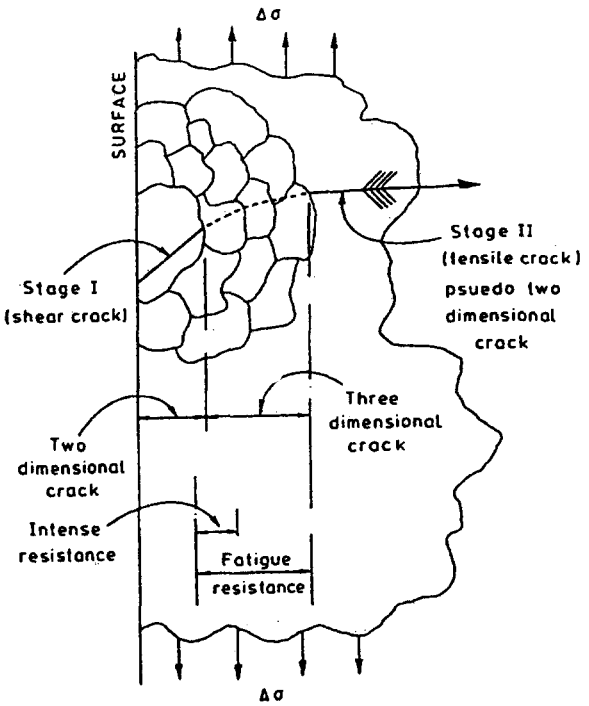

Figure 5. Stage I (shear) to Stage II (tensile) transition for uniaxial cycling [9].

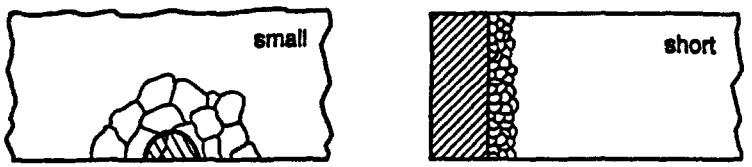

Figure 6. Distinction between microstructurally small cracks (left) and short cracks (right) [10].

implicitly embedded in the classical decomposition of fatigue life in (1), the identification of appropriate mechanics approaches for the lower scales and modeling of the transition from one dominant scale to the next are unsettled topics.

Stage I crystallographic (shear-dominated) microcrack growth is typically observed to transition to the Stage II growth regime for crack lengths on the order of 1 to 4 grain diameters. Figure 5 shows typical crack paths and crack length relative to grain size for uniaxial loading [8–9]. High slip mobility on numerous systems promotes shear decohesion on conjugate slip planes at the crack tip, limiting Stage I coplanar growth and facilitating Stage II growth [9]. This transition depends on stress amplitude and stress state, and its conditions are not yet fully quantified. Propagation of long cracks in initially isotropic polycrystals almost always exhibits Stage II growth, corresponding to mode I dominance.

Because of the distinction of the various length scales and associated mechanics approaches that are necessary, it is essential to define small or short cracks relative to long cracks. The latter may be treated using conventional LEFM in most cases, whereas different approaches must be applied to sufficiently small or short cracks. *Physically small* cracks are those less than 1–2 mm in length. Below this, the notion of 'smallness' is governed by the ratio of crack size to microstructure, as shown in Figure 6 [10]. We consider *microstructurally small or short* cracks

to be those for which the crack length is on the order of periodic microstructure, typically grain size. In some cases, colonies or packets of second phase in dual phase microstructures may define this length scale; in dual phase microstructures, influence of microstructure may persist up to crack lengths an order of magnitude longer than the characteristic grain sizes or mean second phase spacing [11]. As distinguished from short cracks, microstructurally small cracks are those in which the crack length is on the order of microstructure in all dimensions. Microstructurally short cracks are those for which one dimension is on a scale much larger than the repeating microstructure, but with length on the order of microstructure in the propagation direction. In both cases there is ample evidence to suggest that crack-microstructure interactions influence crack growth significantly, with stress state and amplitude also affecting such interactions. Mechanically small cracks are those which are physically small but no longer exhibit significant dependence on microstructure; the crack length for this transition to relative insensitivity is often on the order of 3–10 grain diameters [9, 12]. Mechanically small cracks may be correlated with long crack data using conventional fracture mechanics parameters that account for bulk plasticity and crack closure effects.

To understand the behavior of small cracks in fatigue, we must consider the multiple stages of formation and growth: nucleation, Stage I propagation, transition to Stage II, and mechanically small crack growth. The nucleation problem has been studied rather extensively for single crystals in the context of surface extrusions and intrusions. Suresh [13] outlines the dislocation gating mechanisms that are responsible for the formation of PSBs and creation of microvoids which eventually coalesce to nucleate fatigue cracks. Recent micromechanical models by Venkataraman and colleagues [14–15] have further quantified the crack nucleation process under idealized conditions. Favorably oriented coarse grains tend to preferentially nucleate cracks at PSBs. Much work has focused on LCF behavior. In addition to these extrusion/intrusion processes associated with PSBs, there are many other important mechanisms for crack formation in polycrystals. Often, the HCF nucleation is related to the formation of small cracks at inclusions near free surfaces rather than classical surface extrusions/intrusions. Grain boundary cracks in polycrystals often form at the length scale of the smaller grains near the surface. Pre-existing defects due to manufacture and processing of these materials often lead to microcrack propagation from the outset, particularly in high strength alloys. Surface defects are often introduced in service due to foreign object impact. The HCF problem is particularly sensitive to initial defect size, orientation, and acuity. This paper will therefore focus more on issues related to microcrack propagation than on the nature of initial defects, crack incubation/nucleation, although in some cases such processes might comprise an appreciable fraction of the total fatigue life.

As shown in Figure 7 [9], at low stress amplitudes microcracks exhibit an oscillatory crack growth rate with respect to crack length for cracks in the order of the grain size d which is often observed to be a microstructural barrier associated with a small crack threshold [8–9]. In this figure, Stage I growth is observed to occur for cracks less than a grain size. At sufficiently low stress amplitudes, the cracks arrest at either the first or second grain boundary. As the crack lengthens, the oscillatory behavior diminishes and eventually the crack reaches the so-called elastic–plastic fracture mechanics (EPFM) regime governed by the ΔJ-integral or the LEFM regime governed by ΔK. At crack lengths on the order of 3–10 grain diameters (or other dominant barrier spacings), the da/dN versus ΔJ or ΔK (with closure-modification as appropriate) curves are typically observed to merge with those realized from long crack experiments.

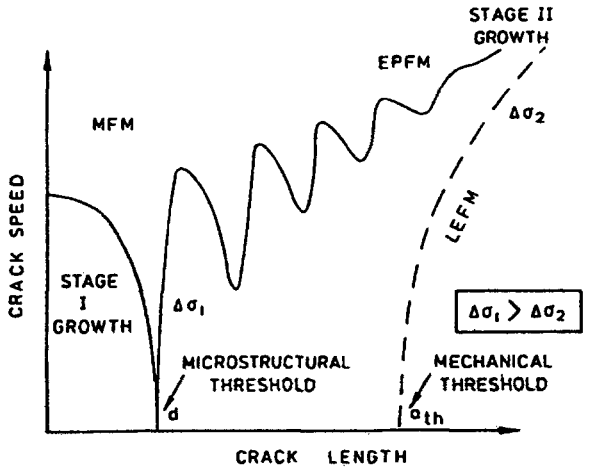

Figure 7. Crack propagation rate versus crack length for microstructurally small to mechanically small cracks [9].

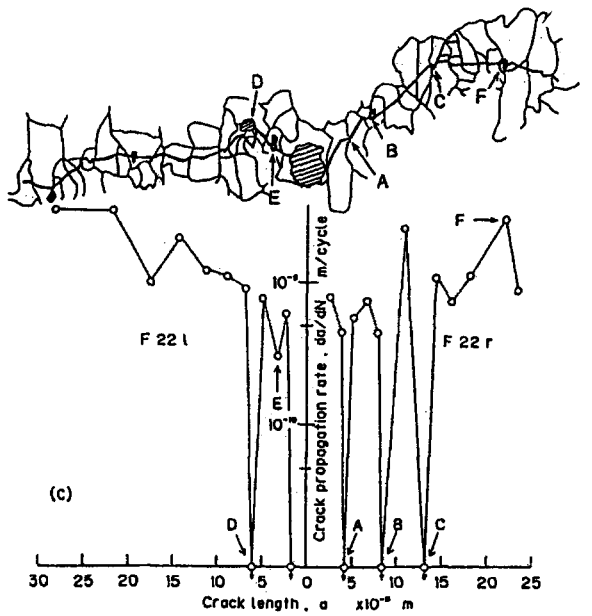

Figure 8. Variation of da/dN versus crack length as dictated by interaction with microstructure for 2024-T3 Al [16].

The oscillatory behavior for microstructurally small cracks arises due to interaction with microstructural barriers. This is shown in the work of Tanaka and Akiniwa [16] in Figure 8, where detailed studies of small cracks in smooth specimens reveal multiple interactions of a growing crack with microstructure for 2024-T3 Al; the crack propagation rate decelerates with crack length upon encountering each obstacle. This leads to the possibility of crack arrest, which may be viewed macroscopically as a fatigue limit or small crack threshold. If the crack length a is less than grain size d the microcrack may be blocked by a grain boundary. If a slip band along which the crack resides does not induce enough stress concentration in the adjacent grain to initiate cyclic slip there (slip transfer), the crack driving force may be insufficient for the crack to bypass the grain boundary. Experimental studies on Al alloys (cf.

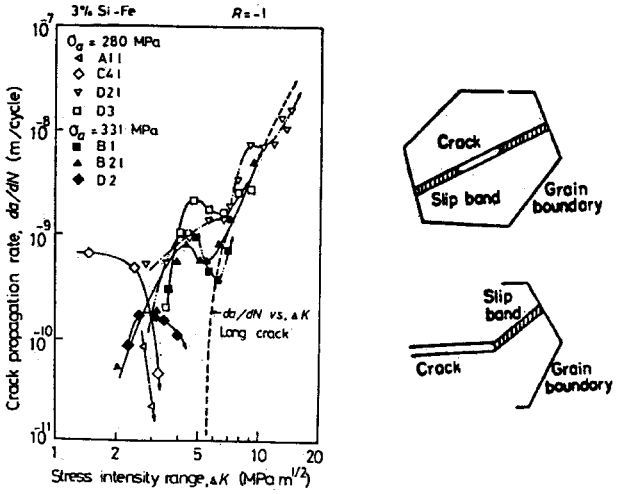

Figure 9. Oscillatory da/dN versus long crack-based ΔK for 3%Si-Fe (left) and (right) schematic of crack/slip band blockage by grain boundaries [18].

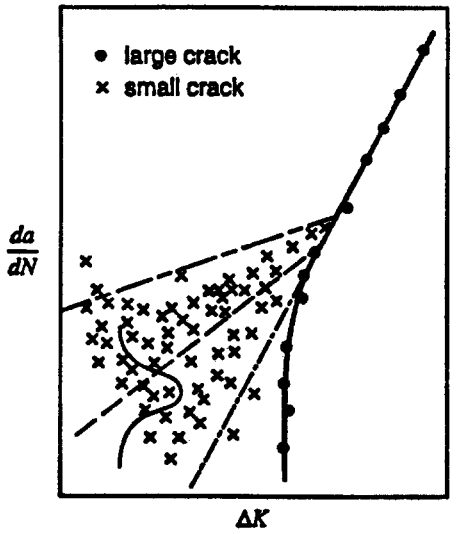

Figure 10. Typical range of da/dN data for small cracks relative to long crack data [10].

[17]) have confirmed that the crystallographic misorientation across grain boundaries plays a key role in the deceleration of small crack growth rate. This type of potential fatigue limit or threshold is important for smooth specimens or in the case of notches of generous radius. Dislocation blockage models have been introduced to quantify this arrest mechanism [18–19]; in these models, crack tip plasticity is represented by distributed dislocations along specific crystallographic planes. Such a threshold may be bypassed completely if pre-existing defects longer than the blockage length scale are present or if there are very sharp notches. As shown in Figure 9 [18], the oscillatory behavior is observed in the da/dN versus ΔK curve for small cracks in a 3%Si-Fe alloy, whereas the long crack behavior exhibits a distinct threshold followed by a Paris growth law regime at higher ΔK levels. The small crack behavior merges into the long crack behavior from above, displaying the characteristic oscillatory behavior.

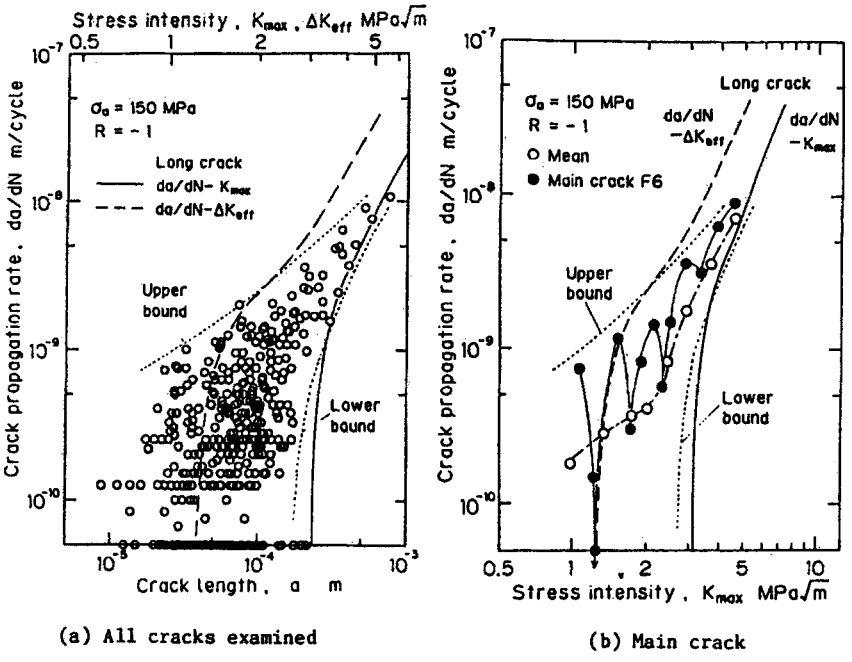

Figure 11. Crack propagation rate for small cracks in 2024-T3 Al versus crack length (left) and $K_{\max}$ (right) [16]. Note the apparent scatter of da/dN for all cracks examined between the lower bound long crack data and the upper bound fully-open curve (da/dN versus ΔK_{eff}).

Rather generically, small crack behavior may be represented within some scatter band at low ΔK levels (below long crack threshold values) as shown in Figure 10 [10]. The apparent high degree of scatter in da/dN for given ΔK may be due both to stochastic effects of microcracks interacting with microstructure as well as deterministic, amplitude-dependent effects. The latter are affected by plasticity-induced closure and crack face interference effects for microstructurally small cracks. Figure 11 shows data from [16] on 2024-T3 aluminum alloy, comparing the lower bound long crack data with crack growth rates for small cracks. Again, significant oscillatory behavior is apparent, associated with microstructural interactions. In Figure 11, the da/dN versus ΔK_{eff} curve represents the behavior of an assumed fully-open crack (no plasticity-induced closure).

For design purposes, it may be expedient to consider that an upper bound exists (as illustrated in Figure 12) for the statistical range of small crack da/dN data when plotted versus ΔK. However, this bound may not prove useful since it is highly conservative, does not acknowledge amplitude and history dependence, and does not admit the possibility of small crack thresholds or non-propagating crack limits.

The Kitagawa diagram shown in Figure 13a [18] illustrates some of the important concepts in threshold limits for the propagation of small cracks in HCF, in this case for a low carbon steel with a ferrite grain size of 55 μm. This diagram essentially represents the locus of points for non-propagating cracks. Three regimes are evident. In Regime I, small cracks do not propagate. Regime I is bounded from above at very small crack lengths by the smooth specimen fatigue limit $\Delta\sigma_{wo}$. In reality, microstructurally small cracks exhibit rather complex oscillatory behavior with propagation at stresses below $\Delta\sigma_{wo}$ (cf. Figure 13b), but eventually arrest if the applied stress amplitude lies below $\Delta\sigma_{wo}$ [8–9, 16], at an upper bound length

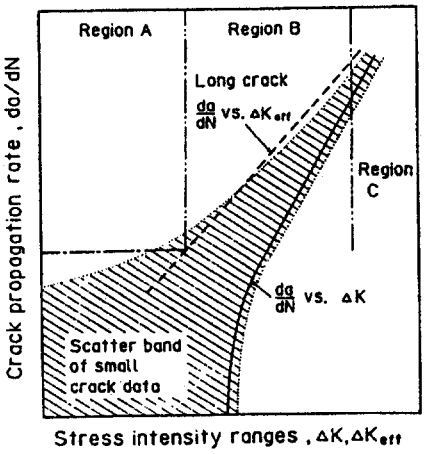

Figure 12. Range of small crack propagation data based on correlation with long crack ΔK solution [16].

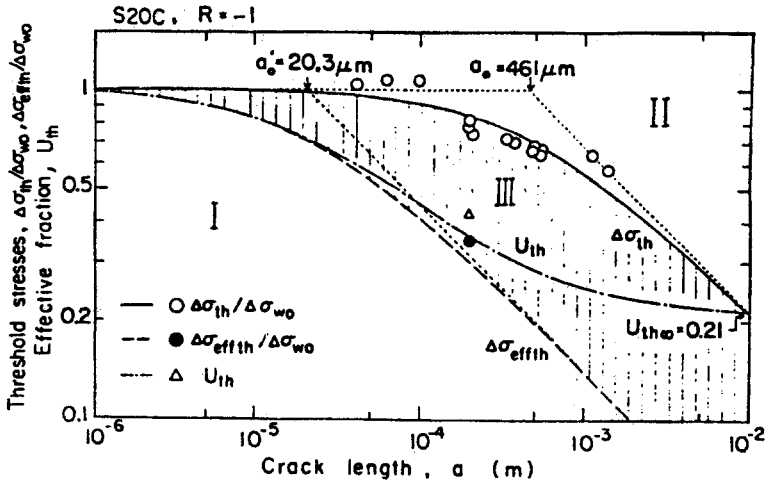

(a)

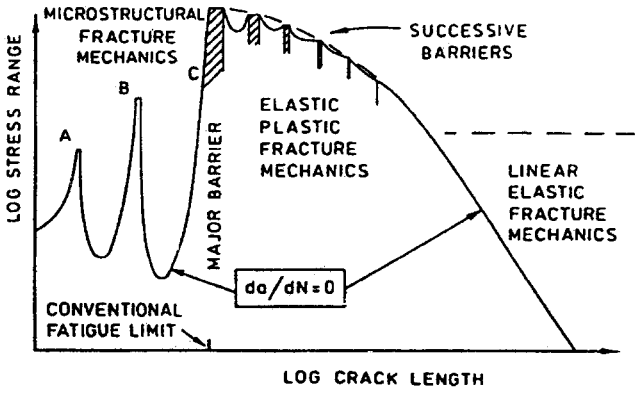

(b)

Figure 13. Kitagawa diagrams: (a) low carbon steel under completely reversed loading [18], and (b) a generic representation which illustrates oscillatory growth behavior for microstructurally small cracks below a_0' or d [9].

given by the dashed curve labelled $\Delta\sigma_{\text{eff th}}$ in Figure 13a. On the other hand, cracks propagate in Regime II at stress amplitudes in excess of the smooth specimen fatigue limit, or at crack lengths which exceed a_0, which is defined as the crack length corresponding to the long crack threshold $\Delta K_{\text{th}\infty}$ based on the smooth specimen fatigue limit. The dashed line limit from a_0 between Regimes II and III corresponds to the long crack threshold of LEFM for $a > a_0$. Clearly, a_0 represents an upper bound on the crack length for non-propagating cracks for stresses in the vicinity of the fatigue limit. Crack length $a_0' = 20.3\,\mu\text{m}$ represents the non-propagating crack limit for microstructurally small cracks; for $a > a_0'$, at stress levels below $\Delta\sigma_{wo}$, small cracks propagate at crack lengths below that of the long crack threshold. This has been attributed to relatively less plasticity-induced closure effects than exist for long cracks in the vicinity of threshold conditions, accounting for the gradual transition from microstructurally small to long crack regimes shown in Figure 13. Cracks in Regime III will grow until arrested at the boundary of Regimes II and III. The construction and interpretation of this diagram has considerable relevance to threshold fatigue design approaches for HCF. The value of such a diagram is that it distinguishes between thresholds for small and long cracks, and to a limited extent the changes of mechanisms as a function of stress amplitude and crack length. However, it is important to point out that such a diagram is applicable to constant amplitude fatigue, and may be significantly altered by overloads or sequences of amplitudes. Hence, it cannot replace detailed incremental models for crack propagation and arrest that consider history effects.

Having mentioned the issue of grain boundary blockage for cracks of length less than the order of the grain size, we consider additional mechanisms which may lead to a fatigue limit in HCF. Elastic shakedown of the heterogeneous cyclic microplasticity response is another source of a fatigue limit, which in general may be lower than that associated with grain boundary blockage of microcracks. There is also a possibility of an elastic–plastic shakedown limit based on insufficient cyclic microplasticity to nucleate cracks. In any case, the consideration of heterogeneity of the polycrystal is essential. For example, the model of Dang Van [20] accounts for the orientation distribution of grains, employing a polycrystal plasticity analysis to assess the intensity of cyclic plasticity and constraint within individual grains. Then, a local critical slip plane failure criterion of Mohr-type, i.e.

$$\frac{\Delta\tau_c}{2} + kP = H \tag{2}$$

is invoked to assess whether the fatigue limit (arrest threshold) of individual grains H is breached. Here, $\Delta\tau_c$ is the range of the maximum resolved shear stress in the grain, and P is the hydrostatic stress. In this manner, shakedown of cyclic microplasticity is explicitly taken into account, although the details of small crack propagation are not considered. Figure 14 illustrates this global/local concept, along with the assessment of the microscopic fatigue criteria [20]. Such local approaches recognize that the description of threshold behavior of local mixed mode I–II nucleation/propagation behavior of Stage I microcracks must consider a combination of maximum shear stress range and some measure of normal stress. This method has successfully correlated HCF life for components such as bearings.

Several other important mechanisms affect the propagation of microcracks in HCF, including crack face interference effects of various sorts. The tip of a Stage I crack inherently involves mode mixity due to the local anisotropic and heterogeneous environment within individual grains. Moreover, Stage I crystallographic growth promotes crack surface roughness-induced interference effects, particularly in low stacking fault energy fcc alloys and for coarse grained

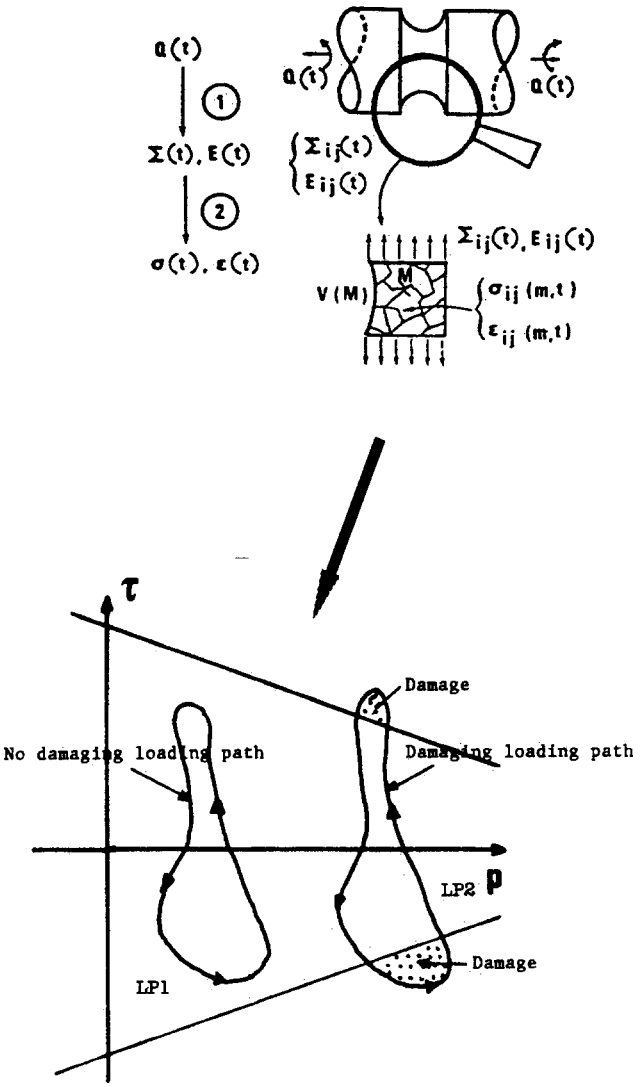

Figure 14. Evaluation of heterogeneous cyclic microplasticity and evaluation of a mesoscale (grain level) failure criterion for HCF [20].

metals. This is particularly important for small cracks in HCF since the distribution of crack-like defects in cyclic plasticity is much less uniform than for LCF condition, and much less deterministic. Invariably, asperities form on crack surfaces for growing small cracks, and these asperities may either bridge or wedge cracks open, leading to local shielding or enhancement. In contrast to LCF, the role of crack face interference becomes increasingly important in Stage I growth under HCF conditions, since mixed mode II–III crystallographic growth is heavily affected by such phenomena and the crack face separation (opening displacement) is very small.

Most of the literature has dealt with mode I crack closure effects. Recent work of Tong et al. [21] addressed modeling of sliding mode crack closure effects due to faceted fracture surfaces which may prevail in Stage I propagation of small crystallographic cracks. This contrasts to plasticity-induced closure transients for both long and short cracks subjected to fairly high

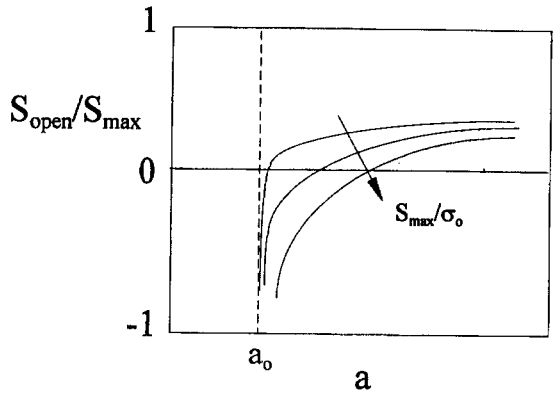

Figure 15. Typical transient in crack opening stress level with cumulative cycles of fully reversed, constant amplitude loading. The nominal opening and maximum stresses are given by S_{open} and S_{max}, respectively, and σ_0 is a measure of the yield strength or flow stress in the elastic–plastic regime. The crack grows from initial crack length a_0 with nearly closure-free conditions at the outset.

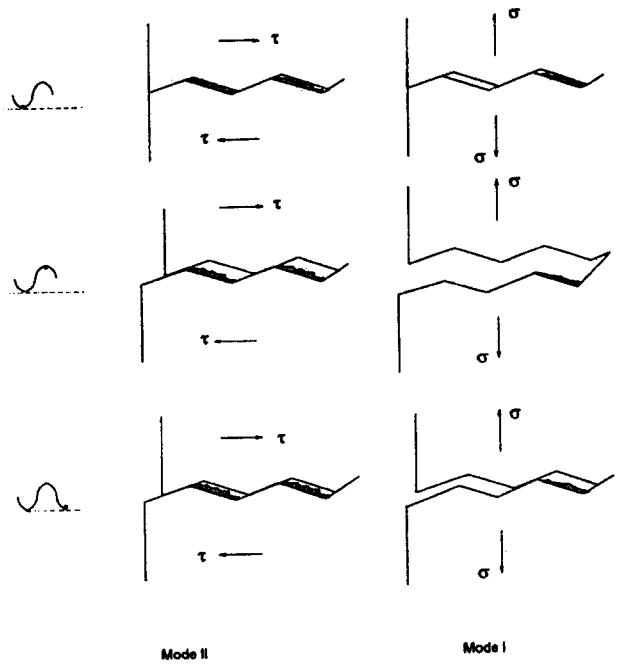

Figure 16. Schematic of microstructural roughness-induced crack interference for mode I and II loading [21].

cyclic strain in mode I, as shown schematically in Figure 15. After suitable crack growth, the crack tip cyclic plasticity generates steady state plastic wake effects which reduce the effective range of stress over which the crack is open [22–23] to some steady level for constant amplitude loading. The precise nature of this transient depends on crack length, load ratio and the crack growth history. Development of plasticity-induced closure prevails in the LCF regime for small cracks, whilst crack surface roughness effects (cf. Figure 16) may become more important in the HCF regime, particularly under Stage I growth where the magnitude of the crack tip sliding displacement is comparable to or exceeds the opening displacement. For small cracks growing in Stage I HCF, an inverted type of closure transient is possible as deduced from the

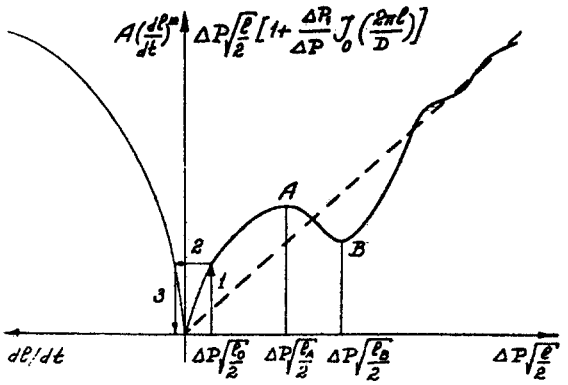

Figure 17. Plot of local $\Delta K = K_{max} - K_{min} = A(d\ell/dt)^m$ versus long crack solution $\Delta K = \Delta P\sqrt{(\ell/2)}$ based on assumption of periodic microstresses ($\Delta P_1 f(x/D)$) superimposed on homogeneous loading, ΔP, where D is the spatial period of the microstructure and ℓ is the crack length [24].

modeling of predominate mode II growth based on frictional contact resistance along the crack faces [21]; in this case, the effective mode II stress intensity factor increases significantly as the crack lengthens, while the effective mode I stress intensity factor decreases. This behavior is quite distinct from that of plasticity-induced closure in mode I. The duration of this transient scales with the ratio of crack length to some microstructural feature length such as asperity height or facet spacing. Eventually, such interactions diminish as the crack lengthens and plasticity-induced closure conditions may be established. It would be interesting to determine if such inverted transients emerge as an outcome of detailed crystal plasticity modeling of asperity contacts. The severity of crack face asperity interactions depends on the nature of cyclic slip in the material, grain size, and even the applied state of stress, as described later.

Another possible source of the oscillatory behavior observed for microstructurally small cracks is the effect of local self-equilibrated residual microstresses that fluctuate at the scale of microstructure, as idealized by Barenblatt [24]. Such microstresses may arise from processing history or as a manifestation of microheterogeneity of elastic properties following local slip. By assigning microstress as a function with periodicity of the microstructure and assuming superposition with the homogeneous applied stress, Barenblatt demonstrated that ΔK became oscillatory with a vastly diminished effect of microstresses after propagation over a few microstructural lengths, as shown in Figure 17, until the long crack solution is approached (dashed line). This simple argument assumes the applicability of long crack mechanics (self-similarity, small-scale yielding, etc.), but clearly demonstrates that residual microstresses may contribute to the oscillatory behavior of small crack driving force and should be considered. The increased driving force for microstructurally small cracks relative to the long crack case is not substantially addressed by this argument. Interestingly, the oscillatory effect due to microheterogeneity of properties is also addressed in dislocation blockage models [18–19], leading to similar conclusions regarding the diminishing effect of microstructure with crack extension. These latter models offer more detailed representation of local mixed mode growth as well.

3. Fracture mechanics parameters for small crack propagation

Variations of standard fracture mechanics theory have been developed for the small crack case in order to address the anomalous rapid propagation behavior of small cracks below the long crack threshold. In appealing to these tools, however, care must be taken to ensure that the self-similarity, homogeneity, and singularity dominance requirements of long crack fracture mechanics apply to the case of small cracks. The guidelines for applicability are vague and the potential for error genuine.

Tanaka and Akiniwa [16] suggested an heuristic approach in which small cracks are assumed to follow the upper bound of the scatter band shown in Figure 12, behaving in accordance with fully open conditions ($\Delta K_{\text{eff}} > \Delta K$), where the da/dN versus ΔK_{eff} curve (dashed line curve in Figure 12) lies well above the long crack da/dN versus ΔK curve. Such an approach is likely to be much too conservative in HCF. Newman [25] performed plasticity-induced closure analyses on small surface cracks at an edge notch for Al 2024-T3, employing the form of long crack ΔK; strong closure transients were predicted in this case as the cracks grew from initial defects (voids) with length on the order of 10–20 μm under initially fully open conditions. The small crack behavior began along the fully open ΔK_{eff} versus da/dN curve, as shown in Figure 18a, and tended towards the long crack behavior as closure developed; thus, plasticity-induced closure evolved through a transient process, analogous to the case of mechanically short cracks growing from elastic–plastic notch root fields.

At lower stress amplitudes, as shown in Figure 18a, a decrease of da/dN was observed as the crack grew away from the nucleating defect. At higher stress amplitudes, on the order of 50 percent of the plastic flow stress level, the da/dN versus ΔK curve was well above that predicted for low stress amplitudes, representing a strong amplitude dependence that arises due to differences in plasticity-induced closure levels. Newman [25] predicted the S-N curve, shown in Figure 18b, assuming a range of initial crack lengths; $R = 0$ and $R = -1$ tests were considered, and the fatigue limit was fit by assuming a threshold level $(\Delta K_{\text{eff}})_{\text{th}}$ of 0.8 MPa$\sqrt{\text{m}}$ for a 20 μm initial crack length. The fully elastic versus elastic–plastic estimates of the driving force were compared, differing substantially only under LCF conditions. Such aluminum alloys tend to exhibit wavy rather than planar slip and may exhibit early transition to Stage II growth behavior, promoting dominance of plasticity-induced closure relative to roughness effects. Comparing Newman's predictions and long crack data in Figure 18 to experimental data for a 2024-T3 alloy with somewhat different long crack da/dN versus ΔK behavior in Figure 11 [16], the oscillatory behavior due to interaction with microstructural barriers is less pronounced in the former since it considers only the initiating defect as a pertinent microstructural feature. Figures 8 and 11 show that grain boundaries play a significant role as well. The mean da/dN versus ΔK behavior is, however, qualitatively similar. Since the small cracks tend to dwell at barriers, the mean da/dN is closer to the valleys of the oscillatory behavior in Figure 11 than to the peaks.

In general, it is unlikely that such an early transition to Stage II will occur, particularly for coarse-grained alloys, or for complex microstructures that do not promote multislip or cross slip. Furthermore, microstructural interactions become much more important under HCF conditions. Inconsistencies in application of long crack fracture mechanics must therefore be addressed. Due to the crystallographic nature of growth of small cracks, there is generally a lack of self-similarity in crack extension; the crack follows a tortuous path with roughness on the order of the crack length itself. The local problem is actually three-dimensional in

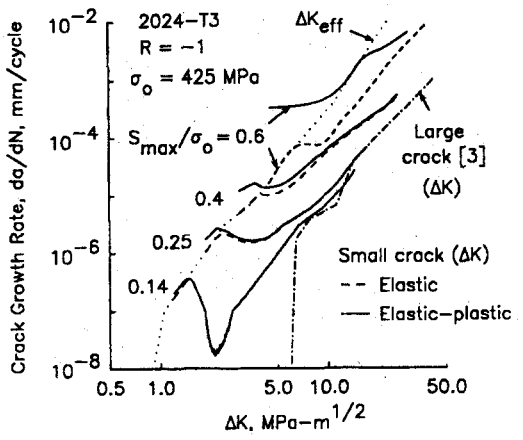

(a)

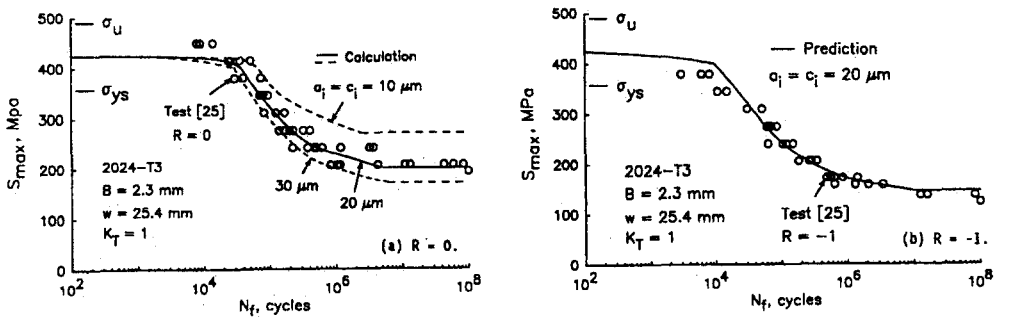

(b)

Figure 18. Treatment of small crack propagation of 2024-T3 using long crack theory with plasticity-induced closure [25]: (a) prediction of da/dN for small cracks for completely reversed fatigue ($R = -1$) compared with long crack da/dN versus ΔK, and (b) prediction of S-N curve for $R = 0$ and $R = -1$ loading.

nature, with local variations of orientation of the crack plane and bowing of the crack front between pinning obstacles. Assumptions of isotropy and homogeneity also do not apply since the crack is embedded in an anisotropic and heterogeneous domain. Singularity-based fracture mechanics breaks down since the scale of crack tip cyclic plastic deformation and the damage process zone may be on the order of the crack length, certainly not well-embedded within a singular field as required for LEFM (or EPFM) applicability.

There are other potentially important effects related to surface proximity for small cracks. The close proximity of the tip of a small crack to a free surface suggests lack of constraint on crack opening and sliding displacements. Slip on planes with components normal to the free surface occurs more easily than it does within the bulk; the effect persists to depths on the order of 5–10 grain diameters [26]. Indeed, grain size, distribution and complexity of microstructure influence the constraint. Small crack constraint calculations in the presence

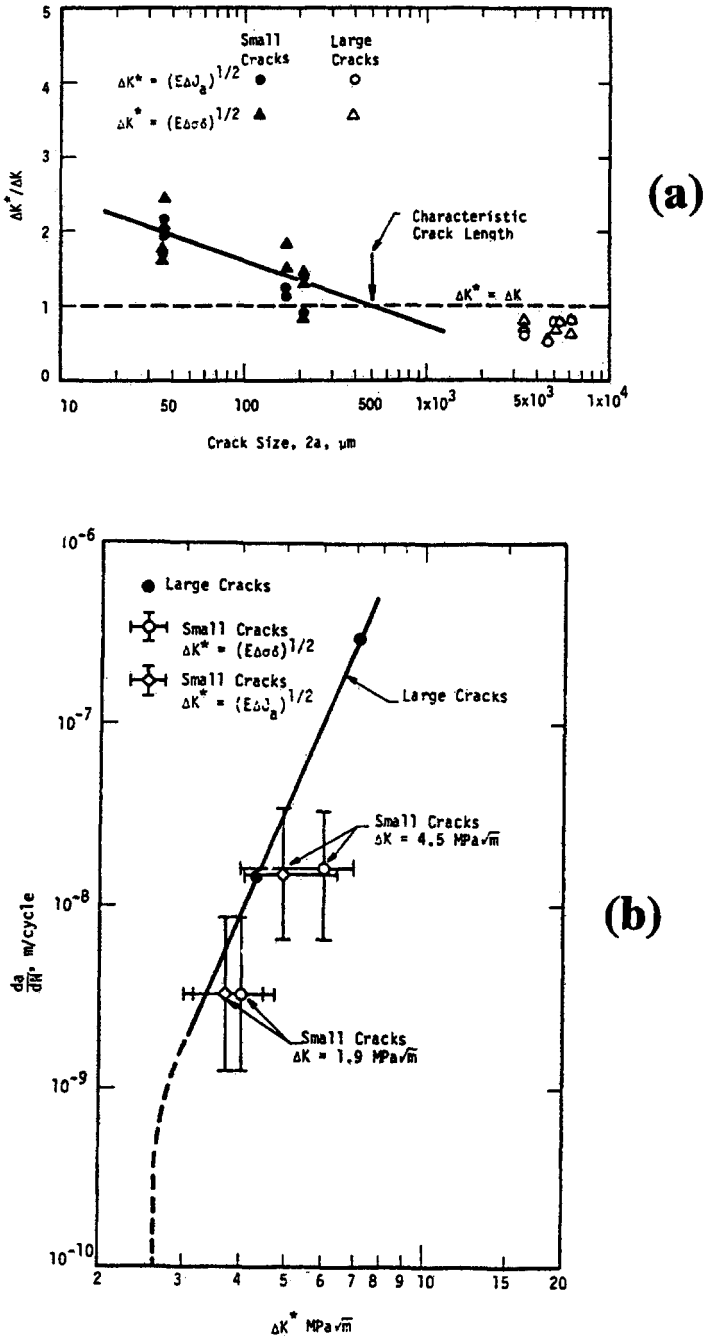

Figure 19. Results of *in-situ* SEM study of Chan et al. [27]: (a) enhanced local ΔJ values ($\Delta K^* = \sqrt{(E\Delta J_a)}$) for small cracks relative to the long crack solution ($\Delta K^*/\Delta K = 1$), and (b) correlation of da/dN for both small and long cracks with ΔK^* for 7075 Al.

of anisotropic microplasticity and microstructure are necessary to quantify constraint effects. This lack of constraint might be expected to contribute to enhanced local crack tip driving forces for small cracks (higher ΔCTOD), for example. Unique experimental data of Chan et al.

[27] illustrate the breakdown of singularity-based mechanics based on long crack solutions, as shown in Figure 19 for 7075 Al. In this work, *in-situ* SEM stereological determination of the local crack tip displacement fields led to 'measured' ΔJ-integral values in the vicinity of the crack tip significantly in excess of those computed using the long crack solution. Furthermore, the measured values of ΔJ were not path independent. In Figure 19a, it is shown that the actual local driving force for the propagation of small cracks ($< 500\,\mu$m) is enhanced by as much as a factor of two for the same remote ΔK relative to that of longer cracks. Furthermore, as shown in Figure 19b, the small crack growth rate correlates with the long crack da/dN versus ΔK^* data when plotted in terms of the local (measured) crack tip opening displacement range (ΔCTOD) or the local ΔJ, suggesting that ΔCTOD is a primal correlative quantity. For the small crack data shown in Figure 19, ΔK^* was based on $\sqrt{(E\Delta J_a)}$, where ΔJ_a was the measured value averaged over the crack tip cyclic plastic zone. Therefore, use of long crack solutions may underestimate the actual crack tip driving forces for cracks of length on the order of several hundred μm and below for this material.

Proximity to a free surface also implies that environmentally-assisted crack propagation mechanisms are potentially of greater concern for small cracks. In fact, the appropriate length scale in this case for definition of a 'chemically small' crack relates to the diffusion penetration depth or chemo-environmental process zone. Small crack growth may be accelerated due to embrittlement ahead of the crack tip, or retarded due to the wedging action of reaction products such as hard oxides which form at elevated temperatures in engine materials, for example [26]. An aggressive environment can also remove the small crack threshold and promote a higher rate of propagation in the microstructurally sensitive regime, thereby effectively eradicating any fatigue limit. Likewise, residual stresses due to machining or processing are highly influential near the surface and must be considered for small cracks. Another aspect of surface proximity is its effect on dislocation accumulation near the surface. Harvey et al. [28] used atomic force microscope images of slip band emergence at the free surface in both HSLA steel and Ti to confirm a model for crack nucleation based on cumulative slip offset which incorporates grain size and other factors; the model is similar in nature to the very different approach of Venkataraman et al. [14–15] based on PSB development. The role of dislocation density gradients in the propagation of small cracks in HCF has not been studied.

It has been suggested that the full elastic–plastic form of the ΔJ-integral based on the long crack solution might account for effects of plasticity at higher stress amplitudes and improved correlation of crack tip driving forces for small cracks. Indeed, mechanically small cracks may be subject to local large scale yielding (LSY) conditions, particularly at higher loading amplitudes. Figure 19a tends to dispel this notion. As seen in Figure 20 [29], it is observed for various polycrystalline metals that microstructurally small cracks exhibit higher propagation rates relative to long crack data when the data are plotted using the long crack ΔJ-integral solution for thumbnail surface cracks. The greatest disparity is observed for the smallest cracks. Neglect of plasticity-induced closure transients in assessing ΔJ for small cracks may also play some role in this discrepancy. Coalescence of multiple cracks is observed for higher da/dN at high cyclic strain amplitudes. In toto, the viability of the long crack solutions for the small crack case is questionable.

One of the hallmark features of microstructurally small crack propagation is deceleration and/or acceleration effects that arise from crack interactions with local microstructure, as shown in Figure 11. There is a subtle distinction of this case from that of interaction of long cracks with barriers. In the latter case, it may be said that the *crack tip* field is influenced by barriers since it is represents a bounded singular domain. For microstructurally small

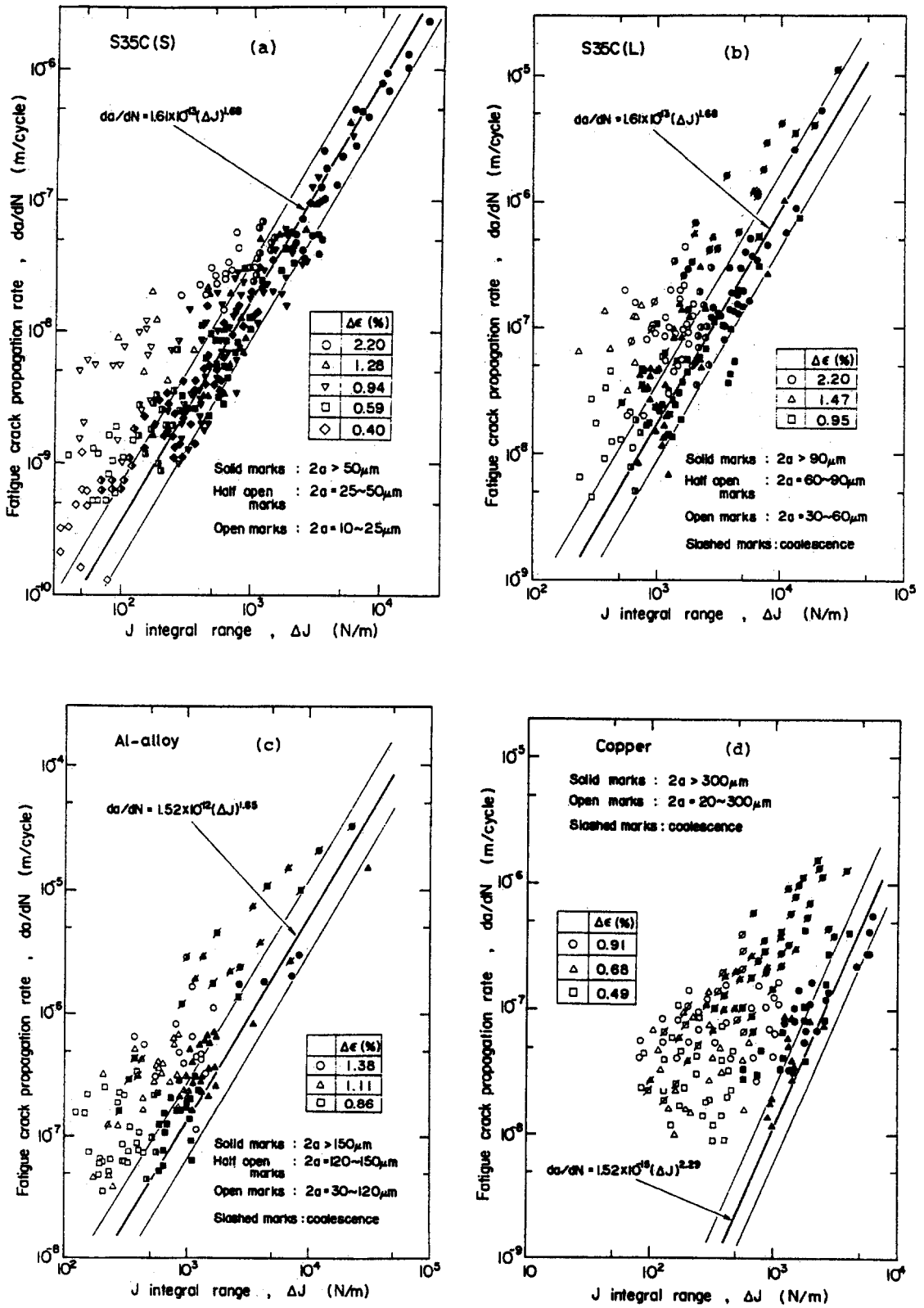

Figure 20. Illustration of elevation of FCP rate for small cracks of various lengths and strain amplitudes relative to long cracks based on the full ΔJ-integral of EPFM for four metals [29].

crystallographic cracks, it is not clear that the tip obeys a singularity of the long crack type since the scale of inelastic deformation, asperity roughness, and damage process zone in the vicinity of the crack may be on the order of the crack length itself. Certainly, the embryonic stages of crack nucleation along PSBs suggests that such cracks embark on growth with the scale of cyclic plasticity and/or distributed damage as the dominant feature. Hence, we may speak of the perturbance of the stress-strain fields in the vicinity of the crack via interaction with microstructural obstacles. In addition to the ab initio application of singularity mechanics, another issue is the viability of roughness-induced closure/obstruction analyses that are based on long crack singularity mechanics when the scale of the contact zone is on the order of the scale of the cyclic plastic zone and the crack length. Detailed microscale analyses are warranted to provide guidelines for an appropriate theoretical construct.

Recognition of these potential limitations of LEFM/EPFM and direct experimental observations have led to alternative small crack propagation approaches. Early on, Tomkins [30] proposed small crack propagation law for LCF based on shear decohesion along conjugate slip planes ahead of a Stage II crack, resulting in linear dependence of da/dN on crack length. In the transition from microstructurally small to long crack behavior, da/dN is often observed to be approximately linear with crack length in LCF. Many of the applications of the ΔJ-integral have been reported for physically small cracks in LCF. Reviews of alternative approaches for microstructurally and physically small cracks may be found in the recent articles of Miller [8–9]. Of particular interest is the recent body of work which has addressed many of the details of microstructural barrier interactions in Stage I and early Stage II propagation. Hobson and colleagues [9, 31] developed empirical laws for deceleration of small cracks approaching a microstructural barrier located at $a = d$, i.e.

$$\frac{da}{dN} = A_0 \tau_a^{\alpha} (d - a) \tag{3}$$

for $a < d$, where τ_a is the amplitude of maximum shear stress, α and A_0 are constants (for a given mean stress), and d is fit by regression analysis of data. Often, d is on the order of a few mean grain diameters, and the average crack growth rate relation in (3) smears oscillatory behavior at individual grain boundaries. For mechanically small cracks, the relation

$$\frac{da}{dN} = B \tau_a^{\beta} a - D \tag{4}$$

was proposed, where D is a threshold growth rate, and B is a constant for a given mean stress. This relation assumes that cracks on the order of 3–10 grain diameters must be treated with an EPFM-type relation due to local LSY effects. The highest rate of either of (3) or (4) is assumed to apply. Arrest may occur if the two curves do not intersect prior to a = d. Figure 21 shows some correlations achieved with small crack data in shear for 2%Ni-Cr-Mo steel [32].

In reality, microstructurally small crack propagation behavior may be viewed as a sequence of intermittent events of bypassing periodic obstacles, consistent with detailed experimental data for cracks on the order of microstructure in length. Navarro and de los Rios [33] have studied the arrest mechanism for Stage I cracks from the perspective of dislocation blockage by grain boundaries, and the capacity to transmit slip to the next grain by activation of dislocation sources therein. In later work, Hussain et al. [34] discuss models of the small crack growth process based on these blockage and slip transfer solutions that display significant microstructural sensitivity and oscillatory growth behavior predicted over the first several grains. The transition to mechanically small crack growth behavior for cracks of length on

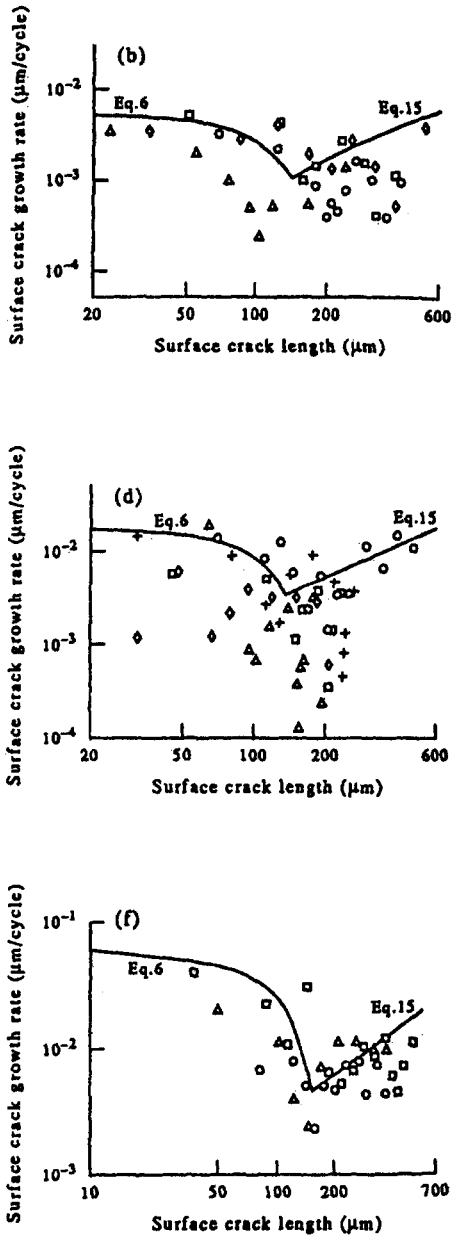

Figure 21. Correlation of small crack growth rate data for 2%Ni-Cr-Mo steel for cyclic shear using (3) and (4) [32].

the order of 3–4 grains for C-Mn steel, considered as the second 'phase' of growth, was shown to occur as a natural consequence of diminishing sensitivity to microstructure [33–34]. Figure 22 presents a comparison of predictions based on this model with experimental data for both phases of growth. Tanaka et al. [35] provide detailed solutions for crack tip sliding and opening displacements which consider grain boundary blockage and slip transfer for Stage I and Stage II microcracks. They show that in addition to grain boundary blockage, large scale yielding and lower effective yield strength near the surface contribute to higher growth rates

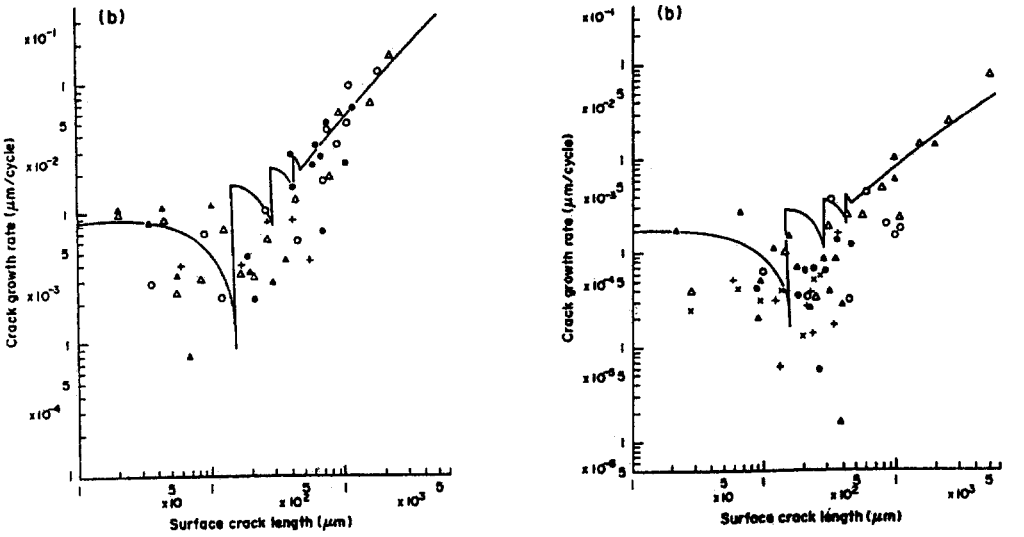

Figure 22. Prediction of propagation behavior of small cracks in simulated HAZ microstructure for C-Mn steel [34] for completely reversed (left) uniaxial loading with $\Delta\sigma = 627$ MPa and (right) torsion with $\Delta\tau = 357.5$ MPa. Different symbols represent different cracks, and the solid curve represents predictions of the two stage propagation model. The average size of ferrite located at grain boundaries is 155 μm; sensitivity to microstructure persists up to 3–4 times this dimension.

for cracks on the order of grain size. Depending on the degree of misorientation with nearest neighbor grains, the first grain boundary may serve as the most effective barrier against arrest, similar to the Hobson [31–32] and Navarro and de los Rios [33–34] models. Local crack closure effects associated with discrete slip bands and crack path fluctuations can also alter the local crack tip opening displacements in Stage II growth, but are not presently well-formulated. While distributed dislocation theory-based approaches offer predictive capability, they are limited in addressing other important effects such as crack branching, lack of constraint associated with proximity to the free surface, and roughness-induced crack face interference.

Tanaka [18] has shown that even in the presence of such periodic interactions, da/dN may be correlated with the crack tip 'highly strained zone' size as determined by the etch-pit technique for 3%Si-Fe, as shown in Figure 23. Superimposed is the same relation for long cracks, suggesting that this relation may be extrapolated to cracks of microstructural length if the various local crack tip opening/sliding shielding and enhancement mechanisms are quantified. These experimental correlations, combined with those of Chan et al. [27], shown in Figure 19, suggest that local crack tip opening/sliding displacements for microstructurally small cracks may provide the necessary 'bridge' to treat both small crack and long crack propagation behavior. Of course, the nature of the highly strained zone/process zone solutions for small cracks in an heterogeneous, anisotropic media differs from that of long cracks. This renders the modeling of the local CTOD/CTSD quite complex. Li [36] presented a detailed vectorial model for cyclic crack tip displacement (CTD), including both sliding and opening components, for Stage I and Stage II cracks in anisotropic elastic–plastic crystals; the FCP rate for aluminum bicrystals correlated well with the local value of CTD. Coplanar slip in Stage I is favorable in the primary PSB for single crystals, high strength alloys with heterogeneous, planar slip or for the first few grains in coarse grain polycrystals, but gives way to multiple

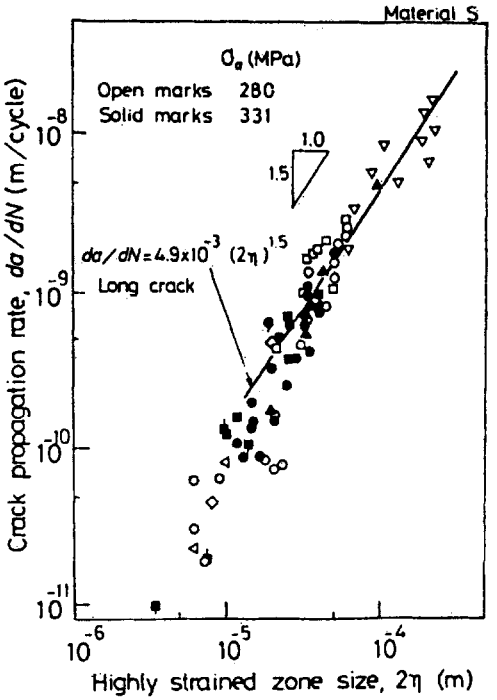

Figure 23. Correlation of da/dN with the highly strained zone size at the crack tip for small cracks in 3%Si-Fe, indicating good agreement with long crack data [18].

slip and Stage II growth on secondary PSB systems as the crack lengthens due to tensile stress concentration and strain hardening along the primary slip band.

This understanding of the distinguishing features of microstructurally small cracks and growing body of local solutions suggests the need to embrace the discipline of *microstructural fracture mechanics or micro-fracture mechanics* for HCF, as suggested by Miller [8–9], in lieu of inappropriately applying long crack solutions; by definition, such solutions are quite material dependent, invoking necessary features of heterogeneity and anisotropy. The previously cited models of [31–36] offer some examples. The central feature of these approaches is the link between crack tip opening and sliding displacements and da/dN.

Another manifestation of the influence of microstructure is the large scatter typical of HCF. This scatter depends on both the distribution of microstructure and of small cracks. Conventionally, probabilistic fatigue mechanics applied at the macroscopic level has considered statistical variation of coefficients and exponents in crack propagation laws to represent stochastic aspects. Weibull statistics have been routinely applied to correlate the scatter of HCF strength in stress-life approaches. Assuming that deterministic correlations hold for small crack growth between da/dN and the local crack opening/sliding displacements or the highly strained zone at the crack tip, it follows that the scatter in microcrack growth rate relates to:

(i) the orientation of the grain(s) in which the crack resides,
(ii) constraint due to neighboring grains of different orientation,
(iii) gradients of surface residual stresses, and
(iv) the spatial distribution and strength of microstructural barriers for a given crack location and geometry.

Tanaka and Akiniwa [16] reported Monte Carlo simulations with variable microstructure that correctly predict the magnitude of scatter of the small crack da/dN using a simple $da/dN = A(\Delta\text{CTOD})^m$ relation, where ΔCTOD is the range of crack tip opening displacement. Hence, a deterministic crack growth law, along with stochastic representation of obstacles, might prove effective in treating the statistical aspects of small crack behavior. Along these lines, Dolinski [37] suggested a growth law of the form

$$\frac{da}{dN} = g(a, \theta), \tag{5}$$

where θ is a set of random variables that reflect the influence of inhomogeneity of microstructure on fatigue properties. In effect, a set of deterministic solutions may be obtained for a range of a set of random variables, and then the realistic variation of these microstructural variables permits assessment of the scatter of da/dN. The average of (5) does not represent the mean crack growth rate, however. This would appear to be the most satisfactory treatment and will require the development of micromechanical solutions for crack interactions with microstructure. Even when certain cracks become arrested at barriers in HCF, others nucleate continuously and must be considered. Hence, the stochastic approach must not only treat the variability of a given crack propagating through a variable microstructure, but of a continuously nucleating family of such cracks.

Finally, an important caveat must be highlighted. Much of our present understanding of small crack behavior has been developed through observations made under predominantly LCF conditions. There are important consequences of low amplitude, HCF conditions which may require a paradigm shift in FCP modeling. Stage I cracks under LCF still have a very significant local mode I contribution in addition to mode II (and perhaps mode III) due to the scale of crack tip plasticity. As previously mentioned, it is expected that the opening displacements diminish in importance relative to sliding displacements under HCF conditions (cf. [13]). In this case, mixed mode I–II roughness-induced interference effects [21] as well as poorly understood mixed mode plasticity-induced closure effects will likely dominate crack growth transients rather than traditional mode I plasticity-induced closure [25] or roughness-induced closure/obstruction concepts based on mode I. In cases where Stage I crystallographic growth is promoted in HCF with little crack surface roughness, small crack arrest at barriers may be quite minimal, with little trace of a small crack threshold. Certain ductile single crystals may exhibit such behavior, for example. As discussed in the next section, the remote stress state also affects the extent of Stage I propagation. Effects of roughness-induced closure transients, crack-microstructure interactions, residual microstresses, and potential arrest behaviors for small cracks in HCF are still open issues.

4. Multiaxial HCF

A discussion of HCF would be incomplete without reference to remote mixed mode loading criteria for small crack nucleation and propagation. Combined stress states are quite common in structural applications. As mentioned earlier, the local conditions at the tip of a Stage I microcrack are mixed mode regardless of the remote loading mode mixity due to crystallographic growth, local anisotropy and constraint of neighboring grains, analogous to bimaterial interface cracks. Therefore, multiaxial behavior in some sense is an inseparable feature of the HCF small crack problem. We may appeal to the previous work in multiaxial fatigue crack initiation mechanics for guidance.

Early works on multiaxial HCF include the extension of the von Mises criterion to the S-N curve and fatigue limit. Haigh [38] recognized that effective stress was inadequate to correlate multiaxial HCF. Gough and Pollard [39] showed that effective stress amplitude was insufficient to correlate HCF under combined bending and torsion, and introduced the ellipse quadrant and ellipse arc concepts for ductile and brittle materials, respectively. An historically common form which has been used to distinguish fatigue crack initiation behavior among stress states is given by

$$\bar{\sigma}_a + g(\sigma_h) = C, \tag{6}$$

where $\bar{\sigma}_a$ is the amplitude of the von Mises effective stress, C is a constant for a given fatigue life, and σ_h denotes either the amplitude or mean value of hydrostatic stress over a cycle. Sines [40] proposed a widely used form in which g is linear in the mean value of σ_h over a cycle. Equation (6) is regarded as a 'universal' relation for fatigue crack initiation which accounts for dependence on stress state. In this section, it will be understood that the term 'fatigue life' pertains to the classical concept of crack initiation, namely the development of a crack of length on the order of 1 mm. The nomenclature N_f will be used interchangeably with N_i in (1).

These modified effective stress approaches have served as the basis for much of engineering HCF design practice during the last four decades. However, they have an indirect relation to the physics of nucleation and propagation of small cracks and do not agree with experimental data in many cases. For example, the completely reversed ($R = \sigma_{\min}/\sigma_{\max} = -1$) uniaxial and torsional fatigue behavior of most polycrystalline metals do not correlate with the effective stress amplitude as suggested by the Sines approach. Experiments show that small cracks propagate on distinct planes in fatigue, following the observations of [7] of Stage I growth. Furthermore, the local crack tip conditions are highly mixed mode in character, regardless of the remote mode mixity. Cracks are sensitive to normal stresses and strains in specific directions, as acknowledged in fracture mechanics. Hence, care must be taken when extending plasticity concepts to fatigue correlations.

In later work, Stulen and Cummings [41], Guest [42], and Findley [43] proposed the earliest forms of so-called critical plane approaches in which the effect of maximum shear stress amplitude $\Delta\tau_{\max}/2$ is modified by the influence of the amplitude of normal stress to that plane $\Delta\sigma_n/2$ i.e.

$$\frac{\Delta\tau_{\max}}{2} + M\frac{\Delta\sigma_n}{2} = G, \tag{7}$$

where M is a scalar multiplier that controls the influence of the normal stress range to the plane of maximum shear, and G is a constant for a given fatigue life. Such correlating parameters, as pointed out by Socie [44–45], are expected to reflect the influence of the normal stress to the crack plane in mixed mode I–II growth under Stage I transgranular growth. The two-parameter approach in (7) is analogous to two-parameter approaches which incorporate constraint effects in fracture through dependence on the degree of triaxiality in addition to the singularity strength. In the present case, the maximum shear stress is assumed as the primary driving force, with additional dependence on the normal stress. Equation (7) belongs to the more general class of Mohr-type approaches for flow and failure of frictional materials.

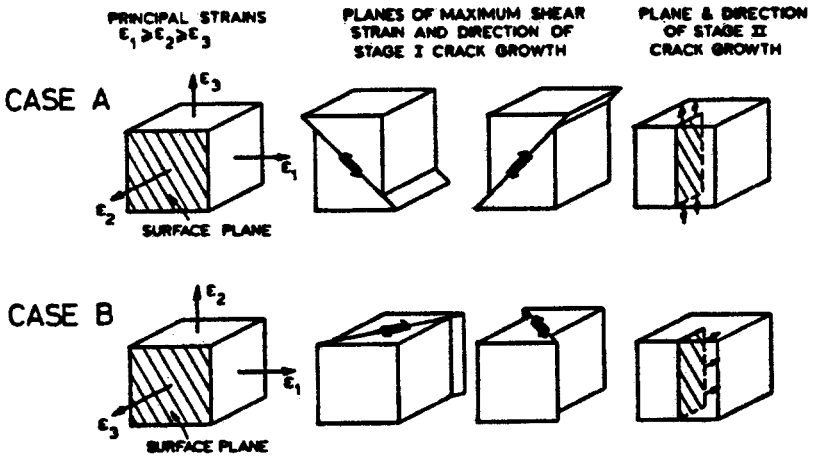

(a)

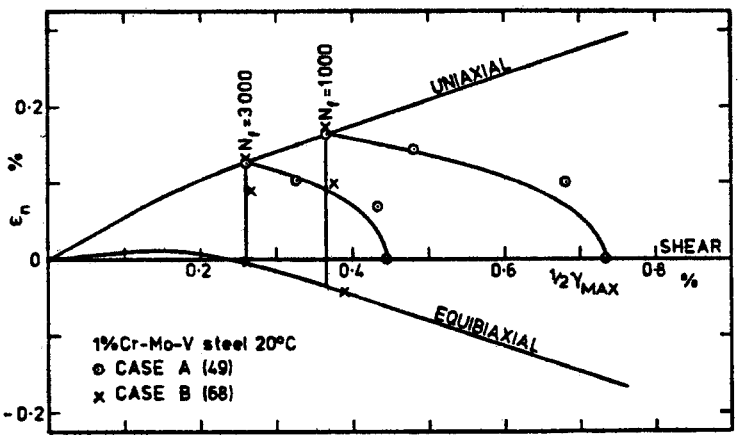

(b)

Figure 24. The distinction between Case A and B cyclic strain states is illustrated in (a) [47]. Typical contours of completely reversed fatigue crack initiation data are presented for 1%Cr-Mo-V at 20°C in the Γ plane in (b), where γ_{max} and ε_n represent amplitudes of maximum shear strain and normal strain to this plane for each case.

With somewhat more emphasis on LCF, Brown and Miller [46] proposed the a two-parameter approach,

$$f_1\left(\frac{\Delta\gamma_{max}}{2}\right) = f_2(\Delta\varepsilon_n) \tag{8}$$

for a given fatigue life, where $\Delta\gamma_{max}$ and $\Delta\varepsilon_n$ are the ranges of maximum shear strain and normal strain to the plane of maximum range of shear strain, respectively, and f_1 and f_2 are nonlinear functions of their arguments. With this set of independent variables, Brown and Miller were able to achieve correlation over a wide range of stress states for both Case A

and Case B type cracking (Figure 24a), using distinct forms for the functions f_1 and f_2 for each case. Case A conditions (e.g. torsion or combined axial-torsion of tubes) are those for which the planes of maximum shear stress or strain lie in the plane of the surface, whereas Case B is defined by these planes penetrating into the surface at some angle (e.g. equibiaxial). Case B is observed to be more damaging (shorter life) for the same $\Delta\gamma_{\max}$. Case A and Case B behaviors are distinctly plotted in the so-called Γ plane in Figure 24b, which serves as a convenient means of representing experimental data using a two parameter approach [47].

Fatemi and colleagues [48–49] introduced a two parameter approach of somewhat different character which has demonstrated robust correlation of fatigue life corresponding to a 1 mm surface crack under various stress states for both Case A and Case B histories, with and without mean stress. This approach is based on the assumption that peak normal stress to the plane of maximum range of shear strain directly affects the Stage I shear-dominated propagation of small cracks. They proposed the correlative parameter

$$\frac{\Delta\gamma_{\max}}{2}\left[1 + K\frac{\sigma_n^{\max}}{\sigma_y}\right] = F(N_f), \tag{9}$$

where K is a constant, $\sigma_n^{\max}$ is the peak normal stress to the plane of maximum shear strain range, and σ_y is the yield strength. Figure 25 presents multiaxial fatigue correlations for both Inconel 718 and 1045 steel using this parameter [50], typically within a factor of two accuracy in fatigue life. Furthermore, Socie [45] has shown that the orientation of microcracking is along the plane(s) associated with the maximum value of this parameter. Most of the correlations obtained to date pertain to LCF or transition fatigue, rather than true HCF. However, the analogy to the HCF relation in (7) suggests more general applicability. Socie [44] has proposed a Smith–Watson–Topper [51] generalization for 'normal stress-dominated' materials, i.e.

$$\sigma^{\max}\frac{\Delta\varepsilon^{\max}}{2} = M(N_f), \tag{10}$$

which may be associated with an early transition to Stage II fatigue crack propagation that was observed to occur under HCF conditions. Li [36] surmised that the sizes of primary PSBs and secondary PSBs for crystallographic cracks depend on the ranges of maximum shear stress and normal stress on the primary slip plane, and play a pivotal role in the selection of extended Stage I growth or transition to Stage II. Equation (9) appears to express dependence on these two quantities, for Stage I and extended Stage I growth, while (10) focuses on predominantly local multislip Stage II tensile growth. Both (9) and (10) involve energy-like products of stress and strain range, structurally analogous but not equivalent to hysteresis energy or ΔJ-integral approaches.

There are fundamental differences between propagation of microcracks in cyclic torsion and tension-compression, as shown in Figure 26 for polycrystalline Inconel 718 [45]. It is clear that propagation of microcracks to a length of 0.1 mm occurs at a much lower fraction of life in cyclic torsion than in cyclic tension-compression. For lives on the order of 10^6 cycles under tension-compression, most of the 'initiation' life is spent with cracks on the order of the grain size. However, in torsion for $N_f = 10^6$ cycles, most of the life is devoted to propagating cracks of length in excess of the grain size. Under LCF conditions, it is apparent from Figure 26 that the propagation of cracks is nearly linear with cycles, assuming an initial crack size on the order of 10–20 μm which is on the order of the size of the smallest grains. These data suggest that crack propagation is only weakly dependent on crack length for high

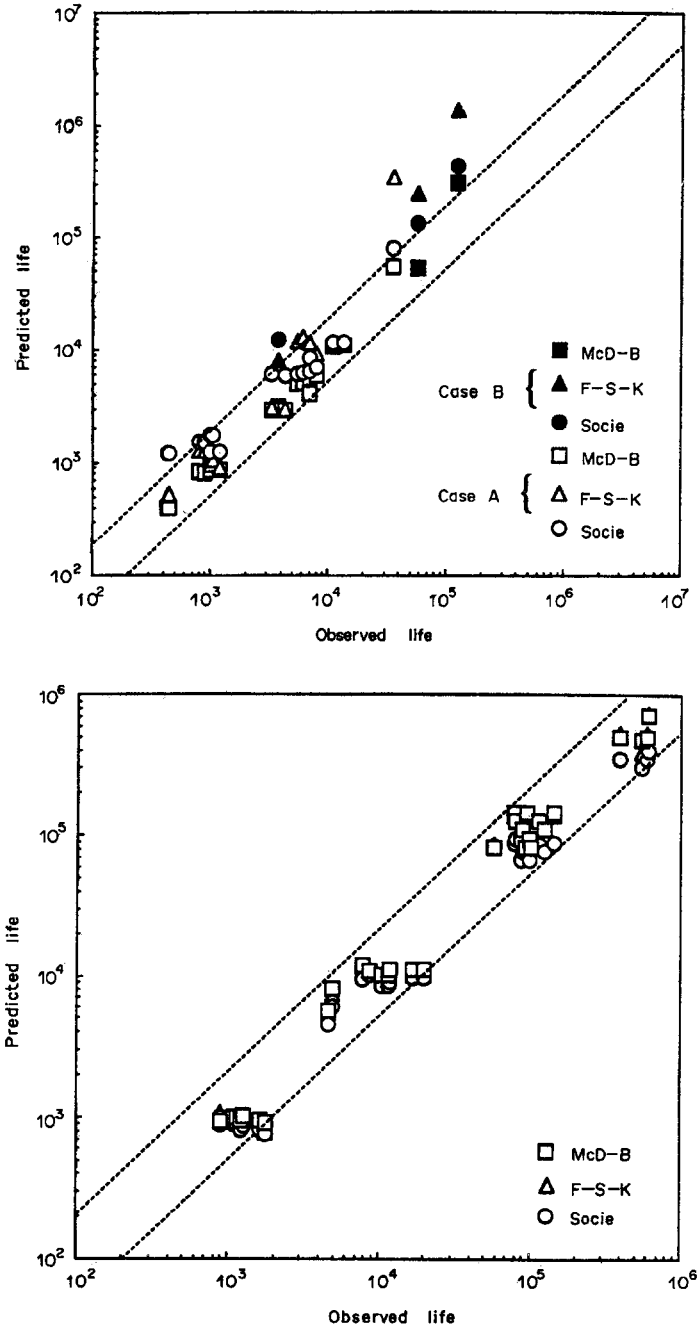

Figure 25. Correlation of Case A and Case B experiments for completely reversed loading of Inconel 718 (left) and 1045 steel (right) [50] based on the Fatemi–Socie–Kurath parameter (F–S–K) [48, 49].

strain amplitudes. At increasing lives, the fraction of life spent in growing cracks less than 100 μm in length increases, to a much greater extent in uniaxial fatigue than in torsional fatigue. The crack growth behavior is quite nonlinear with respect to crack length for cracks shorter than 100 μm under HCF conditions, particularly for uniaxial fatigue at longer lives. There are important implications of the nonlinear growth behavior of small cracks for both

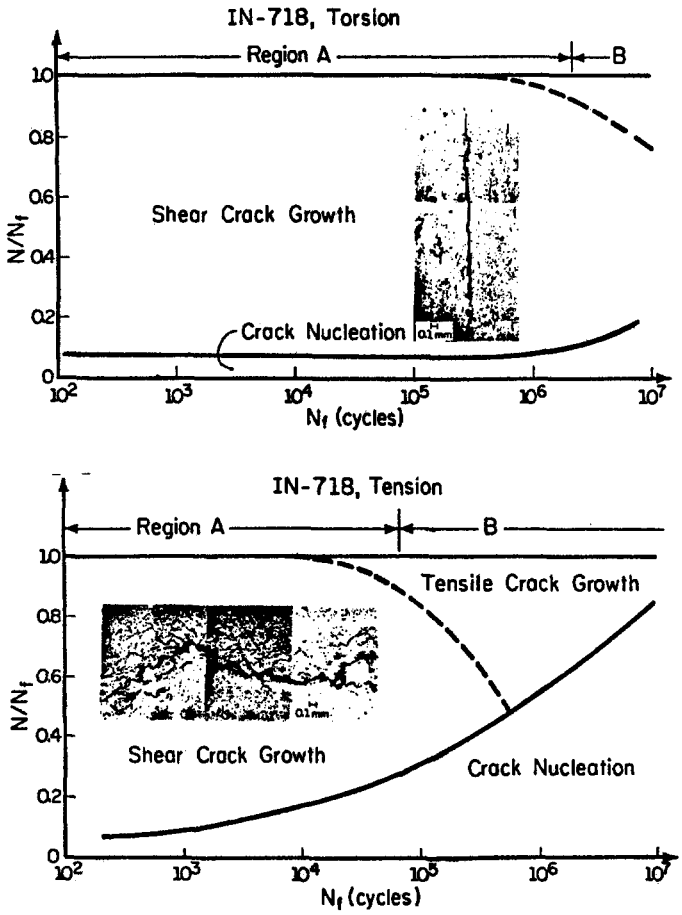

Figure 26. Data of Socie [45] for IN 718 based on number of cycles to 0.1 mm (lower curve) and 1 mm cracks ($N/N_f = 1$) for torsional (top) and uniaxial (bottom) loading.

amplitude and stress state sequence effects, as discussed earlier in connection with Figure 2. Also, the point of departure from Stage I shear-dominated crack growth to Stage II normal stress-dominated growth occurs at higher strain amplitudes for uniaxial fatigue, likely due to the influence of the normal stress across the Stage I crack in promoting secondary slip band formation and crack branching at the crack tip. Torsional fatigue appears to promote Stage I behavior at longer lives for a given crack length, perhaps associated with low symmetry slip (lower Taylor factor and more primary slip) at the local level. This likely points to an enhanced microstructural roughness-induced shielding effect in uniaxial HCF relative to torsion when the crack opening displacement is on the scale of crack surface roughness variation. Iso-crack length contours similar to those in Figure 26 have been constructed for other alloys as well [45], with consistent and similar differences between torsional and uniaxial behavior. Moreover, fundamental differences exist between both of these two stress states and other states such as equibiaxial tension, for example.

Observations under uniaxial loading reveal that small cracks transition from transgranular Stage I growth to Stage II growth when the ratio of crack length to grain size is in the range of 1 to 4 [8–9, 35]. The influence of microstructure is observed to wane during or somewhat after this transition. This transition crack length may also depend on stress state and stress

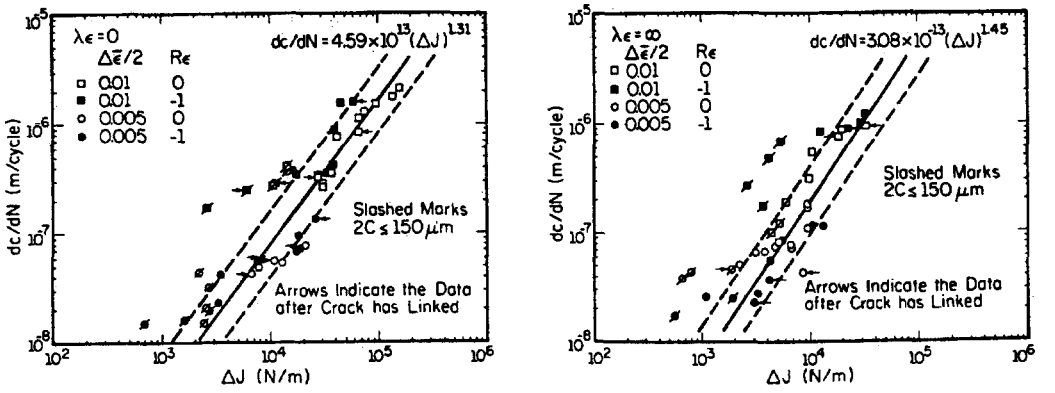

Figure 27. Correlation of uniaxial (left) and torsional (right) fatigue crack growth rate with a mixed mode long crack form for ΔJ [53] for Inconel 718. The growth curves are distinct for the two cases based on ΔJ.

amplitude; these issues are not yet fully resolved. For example, Socie [45] reported almost no perceptible Stage I growth for small cracks in AISI 304 stainless steel in uniaxial fatigue, and for lives in excess of 10^5 cycles in torsional fatigue. This transition is clearly related to the balance of competing local mode I and mode II crack tip displacement mechanisms [52], alluded to in the work of Li [36]. Some modeling efforts have been devoted to the role of grain boundary blockage and transmission of slip to adjacent grains in defining this transition [33].

The applicability of critical plane approaches for shear-dominated microcracking appears to be closely linked with the Stage I propagation phase for small cracks. Hoshide and Socie [53] applied a mixed mode I–II form of the long crack ΔJ-integral of EPFM to combined axial and torsional loading of smooth tubular specimens to correlate the fatigue crack growth rate behavior of small cracks using the power law relationship

$$\frac{da}{dN} = A(\Delta J)^m, \tag{11}$$

where ΔJ in this case was based on a mixed mode I–II form. The exponent m varies somewhat according to stress state. Figure 27 shows the correlation of da/dN data [53] based on (11) for Inconel 718 subjected to uniaxial and torsional fatigue. Reasonable correlation was obtained, although once again it is observed that crack lengths less than 2–3 grain diameters ($< 150\,\mu$m) exhibit a higher growth rate than suggested by the power law relation based on data for longer cracks. As a generalization, Hoshide and Socie [53] recommended the propagation criterion

$$\frac{da}{dN} = A_{\mathrm{I}}(\Delta\delta_{\mathrm{I}})^{m_1} + A_{\mathrm{II}}(\Delta\delta_{\mathrm{II}})^{m_2}, \tag{12}$$

where it is understood that $\Delta\delta_{\mathrm{I}}$ and $\Delta\delta_{\mathrm{II}}$ refer to mode I and mode II crack tip opening and sliding displacement ranges, respectively. While the ΔJ-integral concept has achieved good correlation for both low and high amplitude cycling of mechanically small/short or long cracks, this concept lacks recognition of the heterogeneity, lack of constraint, breakdown of self-similarity and local large scale yielding effects for microstructurally small cracks (cf. [54]). Earlier reference was given to the *in-situ* study of [27] which demonstrated that the measured local ΔJ values for small cracks in 7075 Al (based on either contour integration or opening displacement) exceeded that of the homogeneous, isotropic continuum long crack solution, even for crack lengths up to 10 to 20 times the mean grain size. Clearly, FCP

criteria expressed in terms of remote stress and strain range quantities implicitly assume some nonlinear mapping or transformation to the local values of δ_{I} and δ_{II}. This mapping is even more complex in HCF than LCF, owing to the higher degree of spatial uniformity of cyclic slip in the latter.

Recognizing the need to introduce such a mapping, McDowell and Berard [50] and McDowell and Poindexter [55] generalized the mixed mode I–II approach in (12) to principally address Stage I growth of cracks from microstructurally small to mechanically small conditions under general multiaxial stress states, i.e.

$$\frac{da}{dN} = \Psi_1\left(\frac{\Delta\sigma_{kk}}{R_n}\right)\Psi_2\left(R_n, \frac{\Delta\tau_n}{2}\right)\Sigma(a,\xi) = \widehat{\Psi}(\delta_{\mathrm{I}}, \delta_{\mathrm{II}}, a, \xi). \tag{13}$$

Here, $R_n = \Delta\sigma_n/\Delta\tau_n$, where $\Delta\sigma_n$ and $\Delta\tau_n$ are the ranges of remote normal and shear stress resolved with respect to crack tip coordinates, and n represents the coordinate normal to the crack plane. This plane is assumed to be that of the maximum range of shear strain (stress). The inapplicability of long crack ΔJ was emphasized in this formulation, along with the desire to relate standard strain-life fatigue crack initiation parameters to a growth law for small cracks. In (13), ξ is a length scale (or set of scales) which properly normalizes dependence on crack length with respect to microstructure, demarcating different regimes of microstructure influence. The form of normalization of crack length with these scales may additionally depend on stress amplitude and stress state [56], to account for the relative scale of cyclic microplasticity and/or damage process zone associated with the crack or crack tip. Hence, history dependent effects such as periodic overloads or underloads are conceptually admitted through the ξ. McDowell and Poindexter [55] considered normalization by only a single parameter, $a/(kd)$, where k is the number of grains which define the microstructurally sensitive growth regime, analogous to the two-stage model of Hussain et al. [34], but based on averaging the small crack da/dN behavior in a manner similar to the model of Hobson [31–32]. Based on the notion that local CTOD quantities control small crack growth [16, 27], it is assumed that the multiplicative set of functions ψ_1, ψ_2 and Σ map into $\widehat{\psi}$, which depends on local opening and sliding displacements. Differences between HCF and LCF FCP were addressed [55–56]. Correlation to within a factor of two on N_f was obtained for a wide range of stress states, stress and strain amplitudes for several materials, similar to the correlation achieved with the parameter in (9). Nonlinear amplitude sequence effects were effectively treated. Various sources of crack face interference mechanisms are implicitly embedded in fitting the parameters based on crack initiation experiments conducted under various stress states. In addition to the two parameters $\Delta\tau_n$ and R_n which imply orientation of the crack plane, σ_{kk} is introduced in (13) to reflect constraint of neighboring material (grains) for small cracks. This is increasingly important at longer lives. The dependence on length scales is not explicit in long crack fracture mechanics; in a geometric sense, they are implicitly evident in the limits of applicability of LEFM, where ξ might represent the cyclic plastic zone size or length of the remaining ligament. It is likely that proximity to free surfaces is another explicit length scale of relevance for small cracks.

At present, small crack propagation laws are largely qualitative in nature due to the complexity of the local problem. Clearly, detailed micromechanical approaches that recognize local anisotropy and heterogeneity effects, such as crystal plasticity, will shed light on more appropriate specific forms for such microcrack propagation laws. The length scales in (13) will arise naturally from such solutions. Incorporation of periodic barrier interactions (cf. [33–34]) and non-propagating crack limits or thresholds associated with grain boundary blockage,

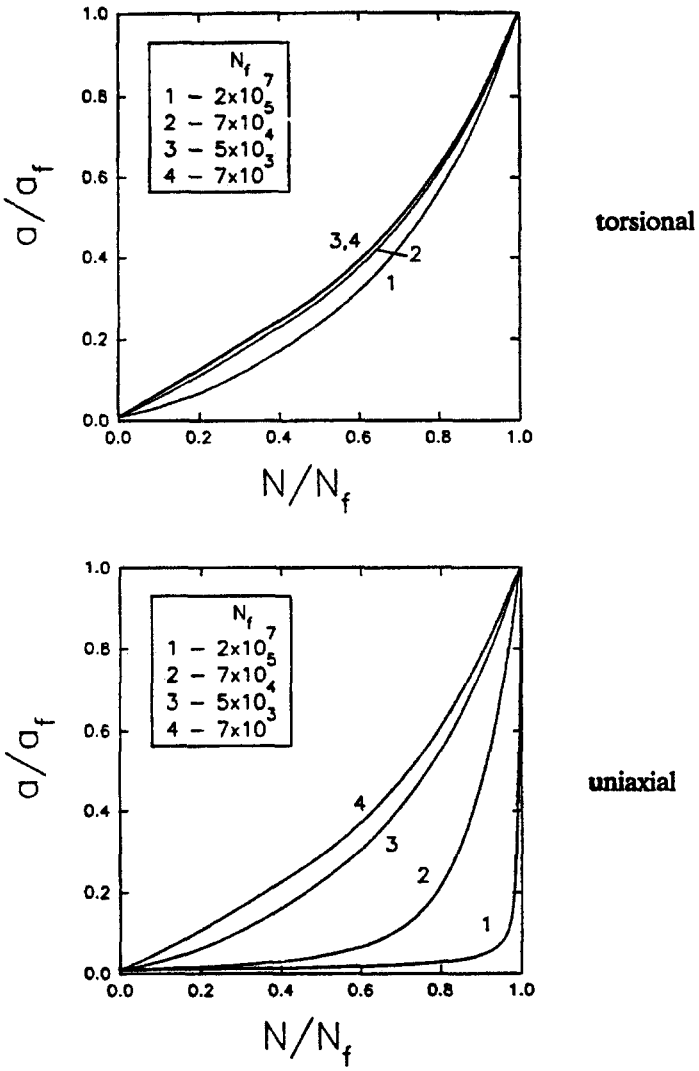

Figure 28. Nonlinear growth of microcracks for 1045 steel in completely reversed torsional fatigue (top) and uniaxial fatigue (bottom) for four different constant amplitude fatigue lives [56].

shakedown of microplasticity, etc. is necessary. Such a framework is consistent with the LEFM/EPFM methodology, even though specific singularity dominance is not asserted. The Stage I–II transition and transition to applicability of the LEFM approach is dictated by satisfying certain criteria that may be expressed in terms of the nondimensionalization of crack length (and perhaps process/plastic zones) by the ξ.

An extremely important aspect is the dependence of the nonlinearity of microcrack propagation on both stress state and stress amplitude. Figure 28 shows normalized crack length versus normalized cycles to failure for lives ranging from thousands to 20×10^6 cycles for 1045 steel. These predictions were made on the basis of the aforementioned McDowell-Berard model, modified to include nonlinearity of da/dN with crack length [55–56]. Data such as those appearing in Figure 26 were fit. Two observations are particularly noteworthy. First, in both uniaxial and torsional cycling, the degree of linearity of crack length with number

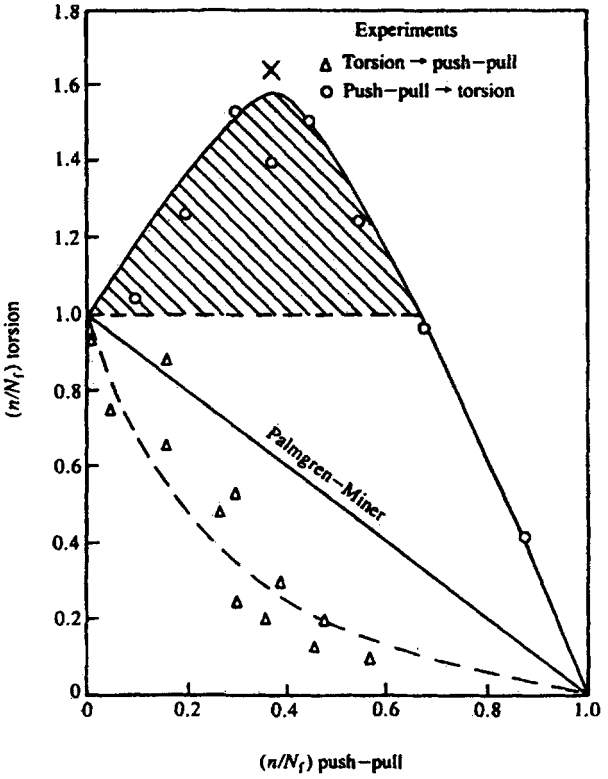

Figure 29. Departure from Palmgren–Miner rule for sequential loading of torsion followed by tension-compression and vice versa [9].

of cycles increases with increasing stress or strain amplitude (LCF conditions). Moreover, uniaxial loading exhibits a much greater dependence on amplitude than does torsion with very low amplitudes characterized by a highly nonlinear crack length versus N relationship. As pointed out in [8, 9], the differences in the nonlinearity of crack growth for small cracks leads to important stress state sequence effects. Figure 29 shows results of sequences of torsional loading followed by uniaxial loading sequence and vice versa [9]. For increasing fatigue life, the departure from Miner's Rule is severe for such sequences and is potentially highly nonconservative.

In summary, critical plane concepts have been introduced to reflect the experimentally observed growth of small cracks under combined stress states. Correlating parameters such as those of (7)–(10) can serve as a basis for constructing small crack growth laws along the lines of (13), particularly when strict limits of LEFM/EPFM applicability are breached. Such laws may provide guidance for development of *microstructural fracture mechanics* principles. Much work remains, however, to establish proper forms of (13) for the HCF case and to derive limits of applicability of LEFM/EPFM for small cracks.

5. Notch effects

Of considerable relevance to HCF is the propagation of small or short cracks from notch root fields where cracks nucleate or where driving forces may be highest for pre-existing defects. Various scales of notches affect the HCF problem. Small cracks can be generated

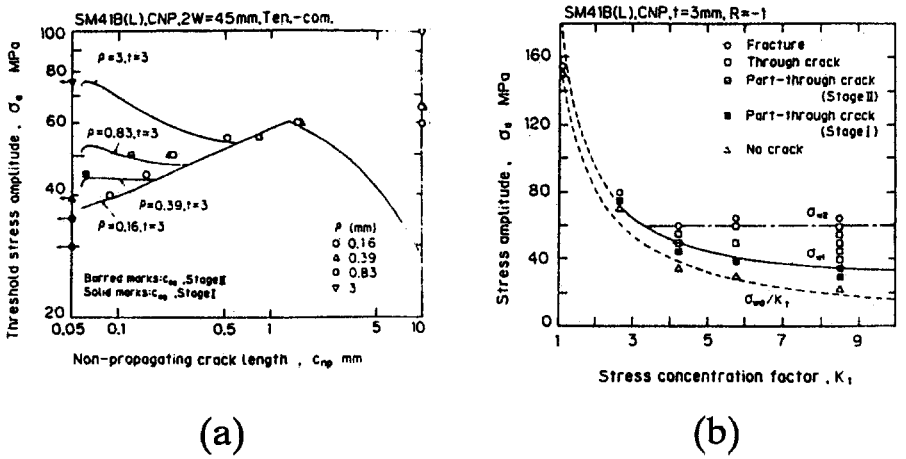

Figure 30. Small crack propagation from notches: (a) limiting curves for non-propagation of fatigue cracks of various lengths in center notched panel specimens for mild steel [16], and (b) relation between fatigue limits and stress concentration for notched specimens.

at micro-notches such as surface damage or near surface inclusions; this process is sensitive to inclusion size, shape factor and orientation relative to the free surface [9]. Usually, HCF failure cracks originate at macro-notches such as holes, fillets, etc.

Tanaka and Akiniwa [16] discuss how the remote applied stress limits for initiation of small cracks and arrest of small cracks depends on notch acuity. It is well-known that notches of small radius may be much less effective in HCF than predicted by the local stress based on the elastic stress concentration factor. This has led to the introduction of the fatigue notch factor K_f in initiation mechanics [6]. Figure 30a shows the threshold stress amplitude curves for non-propagation or arrest of small fatigue cracks in mild steel under $R = -1$ tension-compression loading of center notched panel specimens with various notch root radii ρ for a given notch length $2t$. Clearly, small cracks will be formed for $\rho = 0.83$ mm, for example, at stress levels above 52 MPa, but will arrest as Stage II cracks at lengths on the order of 0.5 to 1 mm. Hence, the fatigue limit for such cracks is controlled by the propagation behavior. For a much larger notch root radius ($\rho = 3$ mm), however, the threshold for forming a Stage I crack is high; stress levels above 75 MPa lead to cracks which are never arrested. Hence, the fatigue limit for larger notch root radii is controlled by the surface fatigue crack nucleation and propagation process. Figure 30b shows the manifestation of these notch root radii effects on the fatigue limit of notched specimens as a function of stress concentration factor K_t, also discussed in [8, 9].

The growth of mechanically small cracks from notches is largely affected by plasticity-induced closure [57]. For example, the work of McClung and Sehitoglu [58] on 1026 steel illustrates that the propagation of mechanically short cracks from notches may be effectively treated using plasticity-induced closure concepts, as shown in Figure 31. In this case, a simple power law dependence of da/dN on ΔJ_{eff} was assumed, where ΔJ_{eff} includes both elastic and plastic contributions to the ΔJ-integral; ΔJ_{eff} is based on $\sigma_{\max} - \sigma_{\text{open}}$, where σ_{open} depends on $\sigma_{\max}$. In these plots, the crack length exceeds five times the grain diameters in all cases. The crack growth transient in this case is due to the change of driving forces as the crack propagates away from the influence of the notch. Likewise Tanaka and Akinawa [16] have shown that the threshold (non-propagating crack) opening stress intensity factor K_{opth} for

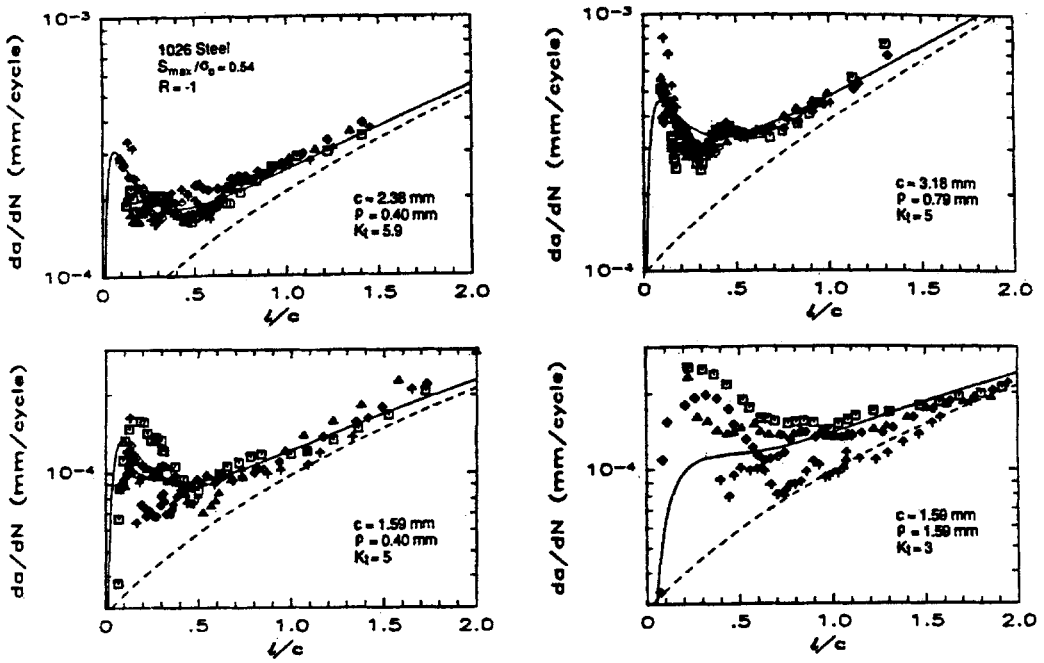

Figure 31. Correlation of plasticity-induced closure effects on da/dN versus crack length for mechanically short cracks growing from notches with a simple short crack model (solid line) that accounts for plasticity-induced closure effects and a long crack model (dashed line) [58].

mechanically small cracks varies from near zero to the steady state value for long cracks with increasing *non-propagating* crack length. This leads to an apparent decrease of the threshold ΔK for smaller cracks. They also showed that the effective stress intensity at threshold, $\Delta K_{\text{eff}} = K_{\text{maxth}} - K_{\text{opth}}$, was essentially constant for mild steel for mechanically small cracks over a wide range of notch dimensions and acuities. This supports the conclusion that crack closure essentially accounts for the differences in propagation of mechanically small and long cracks, as assumed in the approach of [25] for small cracks. For mechanically small cracks growing in a notch root field with significant cyclic plasticity, it is necessary to invoke EPFM concepts to describe closure effects [58]. It should be emphasized, however, that additional factors significantly influence the propagation of microstructurally small cracks in Stage I and early Stage II, as outlined in the previous section; the use of $\Delta K_{\text{eff}}(\Delta J_{\text{eff}})$ is insufficient in such cases due to the various factors that preclude application of LEFM (EPFM) theory. For microstructurally small cracks growing in notch root fields, plasticity-induced closure effects must be augmented by the relevant microstructural interactions ahead of and in the wake of the crack tip. The transition to Stage II growth is affected by notch size and acuity as well. The mechanics of incorporation of crack closure effects for microstructurally small cracks is likely to differ substantially from that of mode I propagation of long cracks.

The Kitagawa diagram of Figure 13 serves as a useful tool for threshold design in HCF, particularly if the details of plasticity-induced closure effects are included in Regime III as shown for propagation of mechanically small cracks below the long crack threshold $K_{\max} < \Delta K_{\text{th}\infty}$. Consideration of micro-notches and growth of microstructurally small cracks from notches complicates HCF analysis relative to the case of mechanically small cracks. The form of the Kitagawa diagram contours for crack lengths of microstructural dimension ($a < a_0'$

in Figure 13) is of critical importance for relatively large notch root radii or for unnotched members. Formulation of a satisfactory theory for microstructurally small cracks growing from notches remains an outstanding problem.

6. Amplitude sequence and mean stress effects

Load sequence effects for FCP of long cracks are reasonably well characterized in terms of models associated with crack tip plasticity based on transient closure and/or stress redistribution effects. Suresh [59] also points out the possible influence of retardation associated with high overload levels due to micro-roughness that arises from the formation of intense shear bands at the crack tip, which may lead to crack branching and residual compressive stresses that induce an effective ΔK level on the order of the threshold. For small cracks in Stage I growth, though, new models must be formulated that account for local heterogeneity, anisotropy, mixed mode growth and nonlinear process zone/plastic zone interactions. Extension of long crack models to this case must be carefully justified to ensure consistency with physical mechanisms. Considering nonlinear evolution of crack length as shown in Figure 28, it is clear that for a given stress state, the Palmgren–Miner rule of linear cycle fraction summation will be particularly inaccurate for sequences of high and low amplitude cycles. Several parametric approaches have been proposed for damage accumulation in the small crack regime (cf. [60]) to describe HCF-LCF interactions; these approaches may serve as a reference for judging consistency of interaction models. For applications where the stress state varies through the history, Figure 28 also indicates that there will be significant nonlinear sequence effects under fully HCF conditions. This has been confirmed experimentally (cf. [8, 9]).

Another important class of amplitude sequence effects not typically relevant in long crack load interaction models is the eradication of fatigue limits (arrest limits) by application of overloads. This affects 'safe' design limits in HCF. If a small crack can effectively bypass the most resistant barrier by breaking a dislocation pileup ahead of the tip through the obstacle or transmitting slip to adjacent grains, it may subsequently propagate at stress levels below the constant amplitude arrest limit. Historically, studies have shown that the fatigue limit in steels, for example, can be 'coaxed' or altered by varying the stress amplitude progressively during an experiment.

Mean stresses are of first order influence in HCF. Empirical design tools have been introduced such as the modified Goodman diagram or similar loci which define 'safe' (non-propagating crack) stress amplitudes for a given mean stress. These laws are based on constant amplitude fatigue experiments at various (constant) mean stress levels. Unfortunately, many practical applications involve sequences of amplitudes and mean stresses. Clearly, mean stress effects in this case are much more complex than indicated by the heuristic Goodman diagram and can render it nonconservative. Invariably, sequence effects are again potentially quite important, since the mean stress effect can be irreversibly altered by prior or periodic LCF. Moreover, engine components experience high frequency, low amplitude stresses superimposed on a high mean stress associated with the overall ground-air-ground cycle. Very little is known about the influence of such high stress ratios in HCF, in addition to effects of LCF/HCF interaction. Preferably, application of incremental crack growth relations which are suitable for each regime of growth will enable prediction of more mechanistically satisfying and reliable fatigue limits. It might be anticipated that high R-ratio experiments in HCF and sequences of HCF-LCF loading will yield much understanding of these important phenomena.

It is important to distinguish between mean stress effects on microstructurally small and mechanically small cracks growing from notches. Tensile mean stress across the plane of Stage I cracks assists propagation for microstructurally small cracks and shortens fatigue life, while compressive mean stress may extend fatigue life for a given stress amplitude [45]. The normal stress to the primary Stage I growth plane affects the crack tip sliding displacement and the rate of propagation [36]. Crack tip shielding effects arise from various sources. As cracks transition to mechanically long status, relatively insensitive to microstructure, plasticity-induced closure and stress redistribution effects tend to dominate; even under compressive mean stresses the crack can grow by virtue of the action of tensile residual stresses in reducing the crack opening stress level [16]. Plasticity-induced closure analyses (cf. [25]) are applicable to such cases.

7. Environment and time-dependent effects

High temperature effects may contribute to HCF failure of engine alloys. Fatigue cracks exhibit transgranular propagation of microcracks at high frequency and intergranular propagation at low frequency. The intergranular mode of crack propagation is due to a combination of creep mechanisms as well as diffusional flow mechanisms, depending on temperature and applied stress level. Microstructural aging under long term exposure poses difficulties in extrapolation of short term test results. It is extremely difficult to conduct experiments in laboratory in a reasonable time frame that reproduce aging and diffusional flow mechanisms realized in actual applications. Also, diffusive penetration of environmental species into the microstructure is known to dramatically affect the fatigue performance of numerous alloys, including Ti alloys and Ni-base superalloys. In addition to these considerations, it is well-known [26] that naturally occurring small cracks may behave quite differently from cracks introduced intentionally via machining processes; the latter may bypass small crack thresholds or microstructure sensitivity exhibited by the former.

The focus over the past 25 years has been on the LCF problem. Creep-fatigue models have been developed including the frequency modified approach of Coffin [2], the strain range partitioning approach [61], damage mechanics and damage curve approaches [62], and explicit crack propagation approaches [63]. Oxidation and environmental effects play a key role in the formation and propagation of microcracks in high temperature alloys. The oxide layer on the surface results in a lack of slip reversibility which serves to enhance the nucleation of cracks. Grain boundaries and slip bands are preferred paths of diffusion, providing ready access to promote growth of short/small cracks. Oxides and various environmental species penetrate ahead of the crack tip, potentially embrittling material in leading to intermittent growth in exposure of new crack surfaces. Moreover, formation of oxides behind the tip may induce crack closure effects that influence the propagation. As pointed out by McDowell et al. [64], it is preferable to adopt approaches which explicitly identify contributions of various mechanisms.

As an extension of creep-fatigue-environment approaches (cf. [63, 65]) to microcrack propagation, Miller et al. [66, 67] have proposed the additive form

$$\frac{da}{dN} = \left.\frac{da}{dN}\right|_{\text{fatigue}} + \left.\frac{da}{dN}\right|_{\text{creep}} + \left.\frac{da}{dN}\right|_{\text{ox}} \tag{14}$$

with

$$\left.\frac{da}{dN}\right|_{\text{creep}} = C_c \widehat{C}^{m_c}, \tag{15}$$

$$\left.\frac{da}{dN}\right|_{\text{ox}} = C_o \left.\frac{da}{dN}\right|_{\text{fat}} \Delta t^{\psi}. \tag{16}$$

The fatigue crack growth rate in (14) is preferably based on an appropriate small crack law; $\widehat{C}$ is a stress power release rate parameter for creep, and C_c, m_c, C_o and ψ are constants.

The additive form of (14) implies an explicit decoupling of the damage mechanisms. However, the deformation mechanisms related to the individual microcrack propagation components may be coupled. As discussed earlier, this type of coupling between creep and fatigue damage may be the most physically relevant for propagation of fatigue cracks. McDowell and Miller [66, 67] obtained correlation for both in-phase out-of-phase thermomechanical fatigue as well as isothermal fatigue tests at different strain rates for MAR-M247 nickel-base superalloy at 500 °C and 871 °C. Such mechanistic approaches, particularly those written in incremental form, are amenable to coupling with fracture mechanics treatment of long cracks under creep-fatigue-environment conditions. For small cracks under thermomechanical fatigue conditions, the emphasis has been on thermomechanical LCF, and future studies must be oriented towards thermomechanical HCF and LCF/HCF interactions. Approaches should distinguish between microstructurally sensitive and insensitive regimes in the case of coupled thermal and environmental effects. In the presence of environmentally assisted crack growth, Stage I propagation may be bypassed completely in favor of Stage II intergranular propagation. Intergranular propagation, if favored, is one Stage II mechanism. Another is the promotion of crack deflection and secondary cracking due to wake oxide interference effects. In some cases, Stage I propagation is resumed as the crack propagates some distance away from the environmentally sensitive surface region. Closure effects arising from various sources should be explicitly considered by such models.

Numerous studies have focused on environmental effects on small crack propagation since the 1960s, and many useful models have been developed. Primarily, effects on LCF and long crack propagation behavior have been addressed. The next generation of models will shift to the formal acknowledgement of microstructural detail and interaction with surface features/gradients for small cracks as discussed in previous sections. Clearly, this represents a challenging area of research and is an important aspect of the HCF problem in high temperature engine components. As mentioned in Section 2, environmental effects have not received primary emphasis here in view of the specificity of mechanisms/models to particular material systems and environments. The reader may find extensive literature for various alloys, pertaining to conditions of most common industrial applications. Herein emphasis is on a common mechanics framework for inclusion of these effects.

8. Summary

Further efforts to improve the accuracy of life estimation of HCF components will need to consider various factors that do not presently exist in either the conventional S-N curve, local stress-life approaches, or traditional LEFM/EPFM approaches. An important consideration is that small/short crack thresholds, if they exist, may be considerably lower than the apparent long crack threshold, leading to non-conservative predictions based on LEFM. Likewise,

loading history effects (e.g. LCF/HCF sequences) and the dependence of initial crack length on crack formation mechanisms present formidable difficulties for simple approaches such as the S-N curve and Goodman diagram.

Numerous basic research issues have been summarized in this article, revolving around the need to consider the local anisotropic, heterogeneous environment of small cracks in HCF. This represents a fertile area of research and development with the objective to develop new hybrid approaches which combine elements of LEFM or EPFM with principles of small crack mechanics. It is envisioned that such a methodology, combined with a realistic, material and application-specific treatment of crack nucleation, would suffice to predict amplitude sequence and mean stress effects in HCF. Moreover, it may ultimately represent extension of damage tolerance concepts to grain size scale defects in critical locations as the resolution of detection methods improve. From a design perspective, probabilistic characterization of initial crack size associated with different mechanisms of crack formation, surface treatment, hardness and residual stress gradients, etc. could be combined with this propagation methodology to provide confidence level estimates of component service life under predominantly HCF conditions. If desirable for a design interface, graphical design tools representing effects of sequence or initial crack size on the life for a crack of certain pre-assigned dimension (e.g. history modified Goodman diagrams or S-N curves) could be derived from this framework. Tremendous progress over the past two decades in computation, material characterization, inspection techniques and projections of future progress in these areas warrant serious consideration of a more detailed treatment of the mechanics aspects of various stages of crack formation and growth in design tools. Present HCF design tools are largely of mid 20th century vintage.

To move in this direction, the following issues must be addressed with regard to small crack propagation models:

- establishment of theoretical limits of applicability of LEFM/EPFM concepts for small/short cracks, including crack length and process/plastic zone scaling as a function of loading condition and material resistance/microstructure
- nucleation of small cracks at surface or near surface defects
- development of appropriate crack tip field parameters for microstructurally small cracks, including interaction with microstructural barriers, micro-residual stresses, slip transfer, and small crack arrest (threshold) or fatigue limits in order to link the opening and sliding displacements with da/dN
- crack tip shielding and enhancement effects for small cracks, with focus on local opening and sliding behavior, and recognizing surface proximity effects
- relation of remote to local mode mixity as a function of applied stress state
- effects of distribution of microstructure/microplasticity on HCF behavior, and linkage to stochastic aspects
- transition from Stage I to Stage II propagation of small cracks
- amplitude sequence effects and cumulative damage analysis, including transcendence and eradication of arrest limits (overload effects for small cracks can reduce, rather than extend, fatigue life)
- combined transgranular/intergranular propagation and effects of environmental penetration

Until the above mechanics issues are addressed in detail, the dichotomy of crack initiation and propagation approaches to HCF will persist. Although not stressed in the present paper, it is clear that detailed modeling of crack tip damage mechanisms and process zones are necessary

to develop specific criteria for crack extension. In view of the small length scales involved, the coupling of continuum solutions with quantum mechanical or molecular dynamical approaches may enhance understanding of microscopic process zone mechanics and propagation criteria in HCF. Studies of surface hardness and residual stress gradient effects of local plasticity due to cyclic loading, surface treatment, and effects of machining, surface impacts, etc. on propagation of small cracks will find a logical place in small crack propagation modeling efforts as well.

Acknowledgements

The author wishes to acknowledge an Air Force Office of Scientific Research-sponsored workshop on HCF held in Dayton, Ohio on June 7, 1995 which stimulated the development of this article. The author is grateful for the support of the Office of Naval Research (ONR N00149510539) for related research.

References

1. P.C. Paris, M.P. Gomez and W.P. Anderson, A rational analytic theory of fatigue, *The Trend in Engineering* 13 (1961) 9–14.
2. L.F. Coffin, A study of effects of cyclic thermal stresses on a ductile metal, *Transactions ASME* 76 (1954) 931–950.
3. S.S. Manson, *Behavior of Materials Under Conditions of Thermal Stress*, NACA Report No. 1170, Lewis Flight Propulsion Laboratory, Cleveland (1954).
4. D.F. Socie, *Estimating Fatigue Crack Initiation and Propagation Lives in Notched Plates Under Variable Loading Histories*, T.&A.M. Report No. 417, University of Illinois (1977).
5. N.E. Dowling, Fatigue at notches and the local strain and fracture mechanics approaches, *Fracture Mechanics, ASTM STP 677*, C.W. Smith (ed.), *ASTM* Philadelphia (1979) 247–273.
6. D.F. Socie, M.R. Mitchell and E.M. Caulfield, *Fundamentals of modern Fatigue Analysis*, Fracture Control Program Report No. 26, University of Illinois, Urbana (April 1977).
7. P.J.E. Forsyth, A Two-Stage Process of Fatigue Crack Growth, *Proceeding, Symposium on Crack Propagation*, Cranfield (1971) 76–94.
8. K.J. Miller, Metal fatigue – past, current and future, *Proceedings, Institute of Mechanical Engineers* 205 (1991) 1–14.
9. K.J. Miller, Materials science perspective of metal fatigue resistance, *Materials Science Technology* 9 (1993) 453–462.
10. R.C. McClung, K.S. Chan, S.J. Hudak, Jr. and D.L. Davidson, Analysis of Small Crack Behavior for Airframe Applications, *FAA/NASA International Symposium on Advanced Structural Integrity Methods for Airframe Durability and Damage Tolerance*, Hampton, VA, May 4–6, NASA CP 3274, Part 1 (1994) 463–479.
11. K. Yamada, M. Shimizu and T. Kunio, Threshold behavior of small cracks in dual phase microstructures, *Current Research on Fatigue Cracks*, T. Tanaka, M. Jono and K. Komai (eds.), *Current Japanese Materials Research*, Elsevier, 1 (1987) 27–40.
12. K. Tokaji, T. Ogawa, Y. Harada and Z. Ando, Limitations of linear elastic fracture mechanics in respect of small fatigue cracks and microstructure, *Fatigue and Fracture of Engineering Materials and Structures* 9(1) (1986) 1–14.
13. S. Suresh, *Fatigue of Materials*, Cambridge Solid State Science Series, Cambridge University Press (1991).
14. G. Venkataraman, T. Chung, Y. Nakasone and T. Mura, Free-energy formulation of fatigue crack initiation along persistent slip bands: calculation of S-N curves and crack depths, *Acta Metallurgica Materialia* 38(1) (1990) 31–40.
15. G. Venkataraman, Y. Chung, and T. Mura, Application of minimum energy formalism in a multiple slip band model for fatigue, Parts I & II, *Acta Metallurgica Materialia* 39(11) (1991) 2621–2638.
16. K. Tanaka and Y. Akiniwa, Propagation and non-propagation of small fatigue cracks, in *Advances in Fracture Research, Proceedings ICF7*, Vol. 2, Houston, TX, (March 20–24 1989) 869–887.
17. Y.H. Zhang and L. Edwards, The effect of grain boundaries on the development of plastic deformation ahead of small fatigue cracks, *Script Metalallurgica Materialia* 26 (1992) 1901–1906.
18. K. Tanaka, Short-crack fracture mechanics in fatigue conditions, *Current Research on Fatigue Cracks*, T. Tanaka, M. Jono and K. Komai (eds.), *Current Japanese Materials Research*, Elsevier, 1 (1987) 93–117.

19. A. Navarro and E.R. de los Rios, An alternative model of the blocking of dislocations at grain boundaries, *Philosophical Magazine* 57 (1988) 37–50.
20. K. Dang-Van, Macro-Micro Approach in high-cycle multiaxial fatigue, *Advances in Multiaxial Fatigue*, ASTM STP 1191, D.L. McDowell and R. Ellis (eds.), ASTM, Philadelphia (1993) 120–130.
21. J. Tong, J.R. Yates and M.W. Brown, A model for sliding mode crack closure: Parts I & II, *Engineering Fracture Mechanics* 52(4) (1995) 599–623.
22. J.C. Newman, Jr., A crack closure model for predicting fatigue crack growth under aircraft spectrum loading, *Methods and models for Predicting Fatigue Crack Growth under Random Loading*, ASTM STP 748, J.B. Chang and C.M. Hudson (eds.), ASTM, Philadelphia (1981) 53–84.
23. R.C. McClung and H. Sehitoglu, Closure behavior of small cracks under high strain fatigue histories, *Mechanics of Fatigue Crack Closure*, ASTM STP 982, J.C. Newman and W. Elber (eds.), ASTM, Philadelphia (1988) 279–299.
24. G.I. Barenblatt, On a model of small fatigue cracks, *Engineering Fracture Mechanics* 28(5/6) (1987) 623–626.
25. J.C. Newman, Jr., A review of modelling small-crack behavior and fatigue-life predictions for aluminum alloys, *Fatigue and Fracture of Engineering Materials and Structures* 17(4) (1994) 429–439.
26. B.N. Leis, A.T. Hopper, J. Ahmad, D. Broek and M.F. Kanninen, Critical review of the fatigue growth of short cracks, *Engineering Fracture Mechanics* 23(5) (1986) 883–898.
27. K. Chan, J. Lankford and D. Davidson, A comparison of crack-tip field parameters for large and small fatigue cracks, *ASME Journal of Engineering Materials and Technology* 108 (1986) 206–213.
28. S.E. Harvey, P.G. Marsh and W.W. Gerberich, Atomic force microscopy and modeling of fatigue crack initiation in metals, *Acta Metallurgica et Materialia* 42(10) (1994) 3493–3502.
29. T. Hoshide, M. Miyahara and T. Inoue, Elastic–plastic behavior of short fatigue cracks in smooth specimens, *Basic Questions in Fatigue: Volume I*, ASTM STP 924, J.T. Fong and R.J. Fields (eds.), ASTM, Philadelphia (1988) 312–322.
30. B. Tomkins, *Philosophical Magazine* 18 (1968) 1041–1066.
31. P.D. Hobson, M.W. Brown and E.R. de los Rios, Two phases of short crack growth in a medium carbon steel, in *The Behaviour of Short Fatigue Cracks*, K.J. Miller and E.R. de los Rios (eds.), EGF Publ. 1, Institute of Mechanical Engineers, London (1986) 441–459.
32. C.H. Wang and K.J. Miller, The effects of mean and alternating shear stresses on short fatigue crack growth rates, *Fatigue and Fracture of Engineering Materials and Structures* 15(12) (1992) 1223–1236.
33. A. Navarro and E.R. de los Rios, A model for short fatigue crack propagation with an interpretation of the short-long crack transition, *Fatigue and Fracture of Engineering Materials and Structures* 10(2) (1987) 169–186.
34. K. Hussain, E.R. de los Rios and A. Navarro, A two-stage micromechanics model for short fatigue cracks, *Engineering Fracture Mechanics* 44(3) (1993) 425–436.
35. K. Tanaka, Y. Akiniwa, Y. Nakai and R.P. Wei, Modelling of small fatigue crack growth interacting with grain boundary, *Engineering Fracture Mechanics* 24(6) (1986) 803–819.
36. C. Li, Vector CTD analysis for crystallographic crack growth, *Acta Metallurgica et Materialia* 38(11) (1990) 2129–2134.
37. K. Dolinski, Formulation of a stochastic model of fatigue crack growth, *Fatigue and Fracture of Engineering Materials and Structures* 16(9) (1993) 1007–1019.
38. B.P. Haigh, *Reports of the British Association for the Advancement of Science* (1923) 358–368.
39. H.J. Gough and H.V. Pollard, The strength of metals under combined alternating stresses, *Proceedings, Institute of Mechanical Engineers* 131(3) (1935) 3–54.
40. G. Sines, Failure of Materials under Combined Repeated Stresses with Superimposed Static Stresses, *NACA Technical Note 3495*, NACA, Washington (1955).
41. F.B. Stulen and H.N. Cummings, A failure criterion for multiaxial fatigue stresses, *Proceedings, ASTM* 54 (1954) 822–835.
42. J.J. Guest, *Proceedings, Institute of Automobile Engineers* 35 (1940) 33–72.
43. W.N. Findley, A theory for the effect of mean stress on fatigue of metals under combined torsion and axial load or bending, *Journal of the Engineering Industry* (1959) 301–306.
44. D. Socie, Multiaxial fatigue damage models, *ASME Journal of Engineering Materials and Technology* (109) (1987) 293–298.
45. D.F. Socie, Critical plane approaches for multiaxial fatigue damage assessment, *Advances in Multiaxial Fatigue*, ASTM STP 1191, D.L. McDowell and R. Ellis (eds.), ASTM, Philadelphia (1993) 7–36.
46. M.W. Brown and K.J. Miller, A theory for fatigue failure under multiaxial stress–strain conditions, *Proceedings, Institute of Mechanical Engineers* 187(65) (1973) 745–755.
47. M.W. Brown and K.J. Miller, Two decades of progress in the assessment of multiaxial low-cycle fatigue life, *Low Cycle Fatigue and Life Prediction*, ASTM STP 770, C. Amzallag, B. Lei, and P. Rabbe (eds.), ASTM, Philadelphia (1982) 482–499.

48. A. Fatemi and D. Socie, A critical plane approach to multiaxial fatigue damage including out of phase loading, *Fatigue and Fracture of Engineering Materials and Structures* 11(3) (1988) 145–165.
49. A. Fatemi and P. Kurath, Multiaxial fatigue life predictions under the influence of mean stress, *ASME Journal of Engineering Materials and Technology* 110 (1988) 380–388.
50. D.L. McDowell and J.-Y. Berard, A ΔJ-based approach to biaxial fatigue, *Fatigue and Fracture of Engineering Materials and Structures* 15(8) (1992) 719–741.
51. R.N. Smith, P. Watson and T.H. Topper, A stress–strain parameter for fatigue of metals, *Journal of Materials* 5(4) (1970) 767–778.
52. M.W. Brown, K.J. Miller, U.S. Fernando, J.R. Yates and D.K. Suker, Aspects of multiaxial fatigue crack propagation, *Proceedings International Conference on Biaxial/Multiaxial Fatigue*, St. Germain en Laye, France (May 31–June 3, 1994) 3–16.
53. T. Hoshide and D. Socie, Mechanics of mixed mode small fatigue crack growth, *Engineering Fracture Mechanics* 26(6) (1987) 842–850.
54. H. Nisitani, Behavior of small cracks in fatigue and relating phenomena, *Current Research on Fatigue Cracks*, T. Tanaka, M. Jono and K. Komai (eds.), Current Japanese Materials Research, 1, Elsevier (1987) 1–26.
55. D.L. McDowell and V. Poindexter, Multiaxial fatigue modelling based on microcrack propagation: stress state and amplitude effects, *Proceedings International Conference on Biaxial/Multiaxial Fatigue*, St. Germain en Laye, France (May 31-June 3, 1994) 115–130.
56. D.L. McDowell, Multiaxial fatigue modelling based on microcrack propagation, *Symposium on Material Durability/Life Prediction modeling*, ASME PVP-Vol. 290, ASME Winter Annual Meeting, Chicago, IL (Nov. 6-11, 1994) 69–83.
57. A.J. McEvily and K. Minakawa, On crack closure and the notch size effect in fatigue, *Engineering Fracture Mechanics* 28(5/6) (1987) 519–527.
58. R.C. McClung and H. Sehitoglu, Closure and growth of fatigue cracks at notches, *ASME Journal of Engineering Materials and Technology* 114 (1992) 1–7.
59. S. Suresh, Crack growth retardation due to micro-roughness: a mechanism for overload effects in fatigue, *Scripta Metallurgica* 16 (1982) 995–999.
60. S.S. Manson and G.R. Halford, Re-examination of cumulative fatigue damage analysis – an engineering perspective, *Engineering Fracture Mechanics* 25(5-6) (1986) 539–571.
61. T. Kitamura and G.R. Halford, A Nonlinear High Temperature Fracture Mechanics Basis for Strainrange Partitioning, *NASA TM* 4133 (1989).
62. J.L. Chaboche and P.M. Lesne, A nonlinear continuous fatigue damage model, *Fatigue and Fracture of Engineering Materials and Technology* 11(1) (1988) 1–17.
63. L. Remy, Recent developments in thermal fatigue, *Proceedings International Seminar on the Inelastic Behaviour of Solids Models and Utilisation, MECAMAT*, Vol. IV (1988) 1–19.
64. D.L. McDowell, S.D. Antolovich and R.L.T. Oehmke, Mechanistic considerations for TMF life prediction of nickel-base superalloys, *Nuclear Engineering Design* 133 (1992) 383–399.
65. A. Saxena and B. Gieseke, Transients in elevated temperature crack growth, in *High Temperature Fracture Mechanisms and Mechanics*, EGF6, B. Bensussan and J.P. Mascarell (eds.), Mechanical Engineering Publications, London (1990) 291–309.
66. M.P. Miller, D.L. McDowell and R.L.T. Oehmke, A creep-fatigue-oxidation microcrack propagation model for thermomechanical fatigue, *ASME Journal of Engineering Meterials and Technology* 114(3) (1992) 282–288.
67. M.P. Miller, D.L. McDowell, R.L.T. Oehmke and S.D. Antolovich, A life prediction model for thermomechanical fatigue based on microcrack propagation, *ASTM STP 1186*, ASTM, Philadelphia (1993) 35–49.